An Introduction to Extratropical Transition

温帯低気圧化入門

Wataru Yanase

(Meteorological Research Institute)

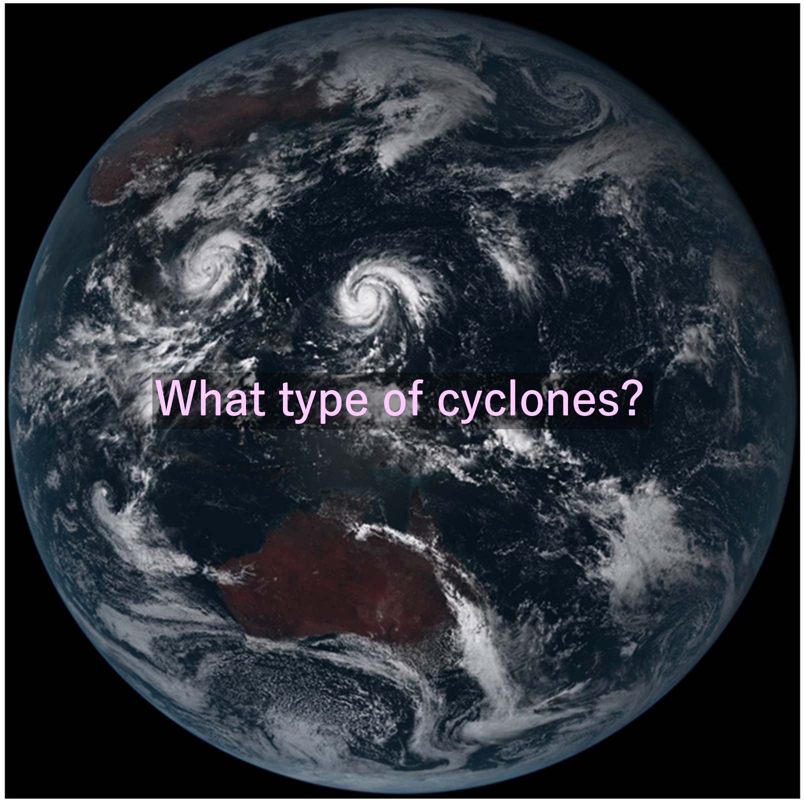

- ✓ I will give an introduction to extratropical transition and cyclone phase space in Japanese, which are the main topics of the lecture by Prof. Hart this afternoon.
- ✓ I attempt to focus on general topics, while I partly present my own motivations and studies.
- ✓ As my foretooth was broken by tough food last week, I have a little difficulty in pronouncing “f” and “v” today.

Typhoon Seminar (DPRI, Univ. of Kyoto, 18–19 March 2024)

Topics

1. Diversity of cyclones
2. Extratropical transition (ET)
3. Cyclone Phase Space (CPS)
4. ET around Japan
5. Cyclone structures during ET
6. An idealized experiment on ET

1. Diversity of Cyclones

低気圧の多様性

Various types of cyclones form around Japan.

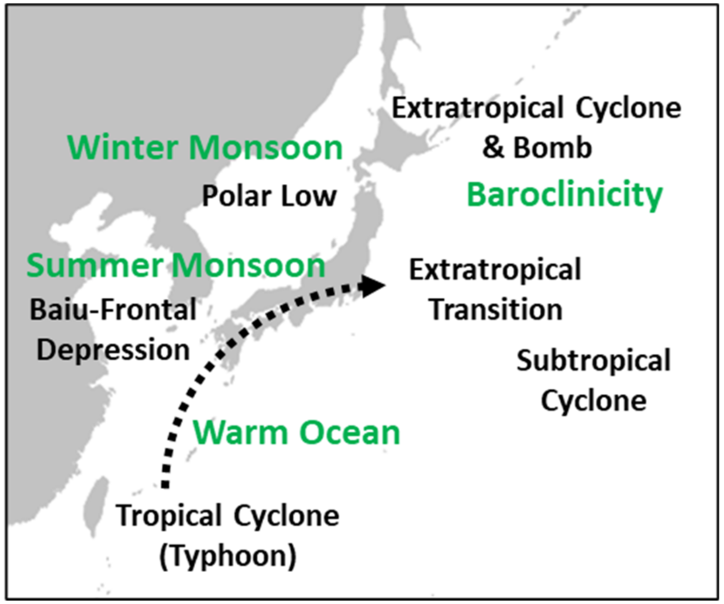

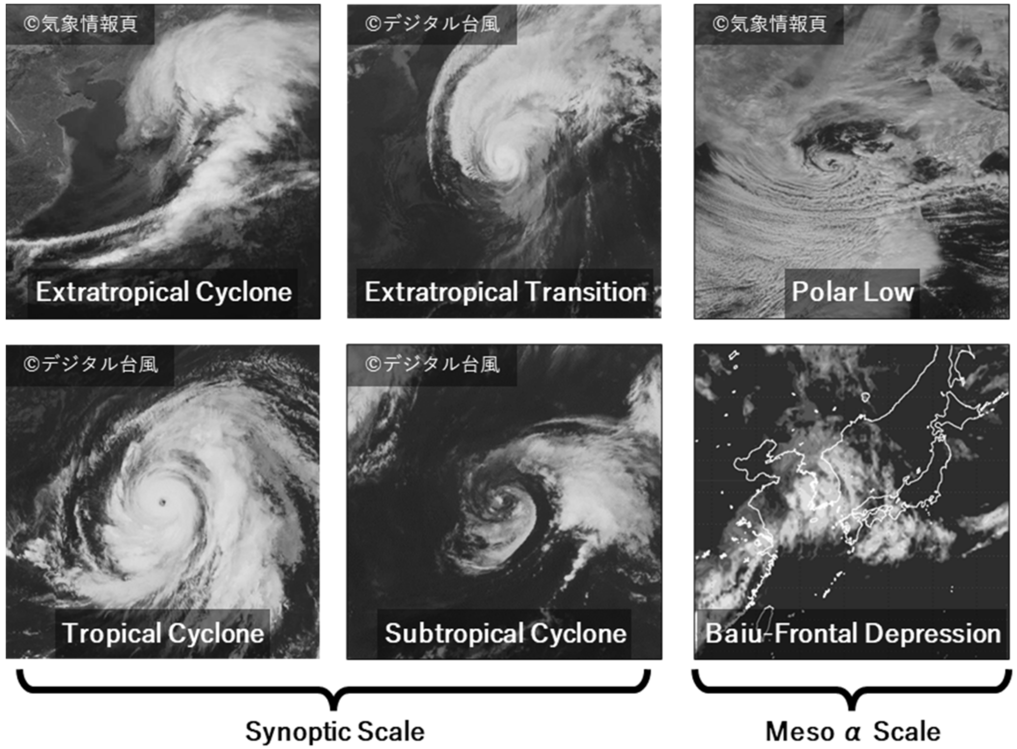

A typical tropical cyclone and an typical extratropical cyclone, two major cyclones, are different from one another.

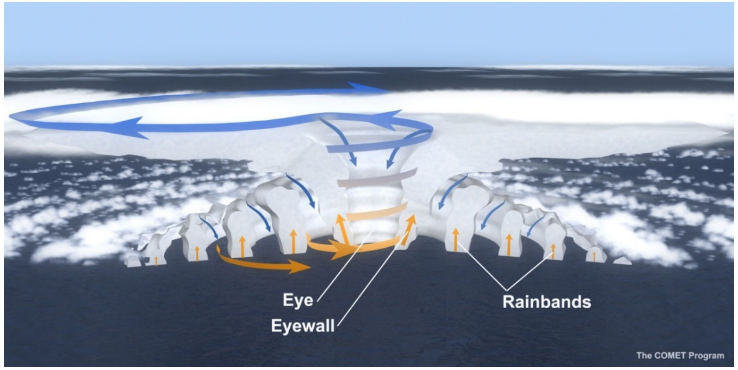

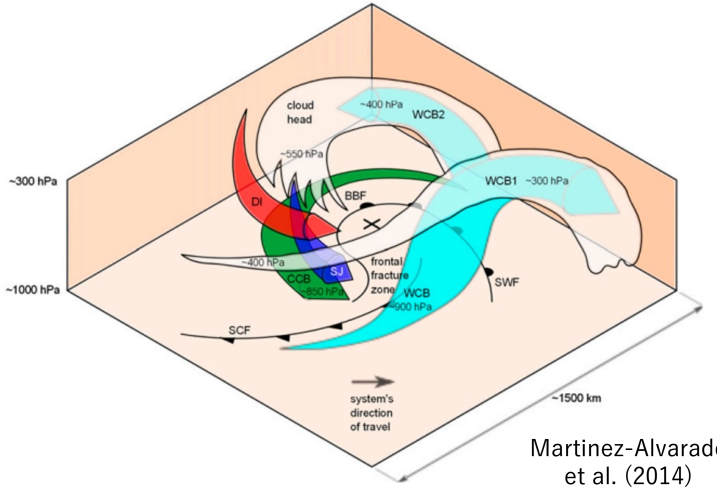

Martinez-Alvarado et al. (2014)

Tropical Cyclone (TC)		Extratropical Cyclone (EC)
Upright vortex	Vortex structure	Westward-tilted vortex
Warm core	Thermal structure	Warm/cold fronts
Condensational heating (diabatic)	APE source	Heat transport (baroclinic)
Warm ocean at low latitudes	Environment	Baroclinicity at mid-latitudes
Interaction between a vortex and diabatic heating (e.g., CISK, WISHE)	Basic theory of intensification	Interaction between upper- and lower-level PV anomalies

Some cyclones are hybrid types.

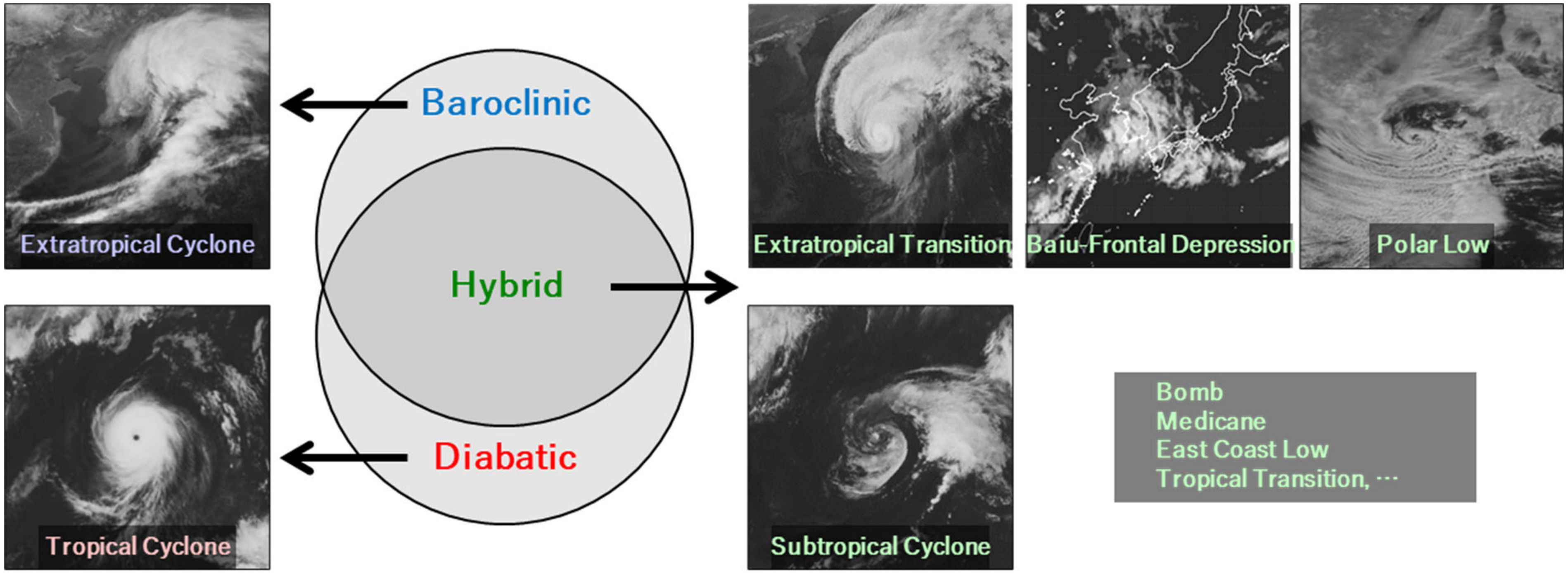

In this talk, a “hybrid” cyclone simply means any cyclone that form through both diabatic and baroclinic processes.

Each type of cyclones also shows a variation:
e.g., the polar low spectrum (Rasmussen and Turner 2003).

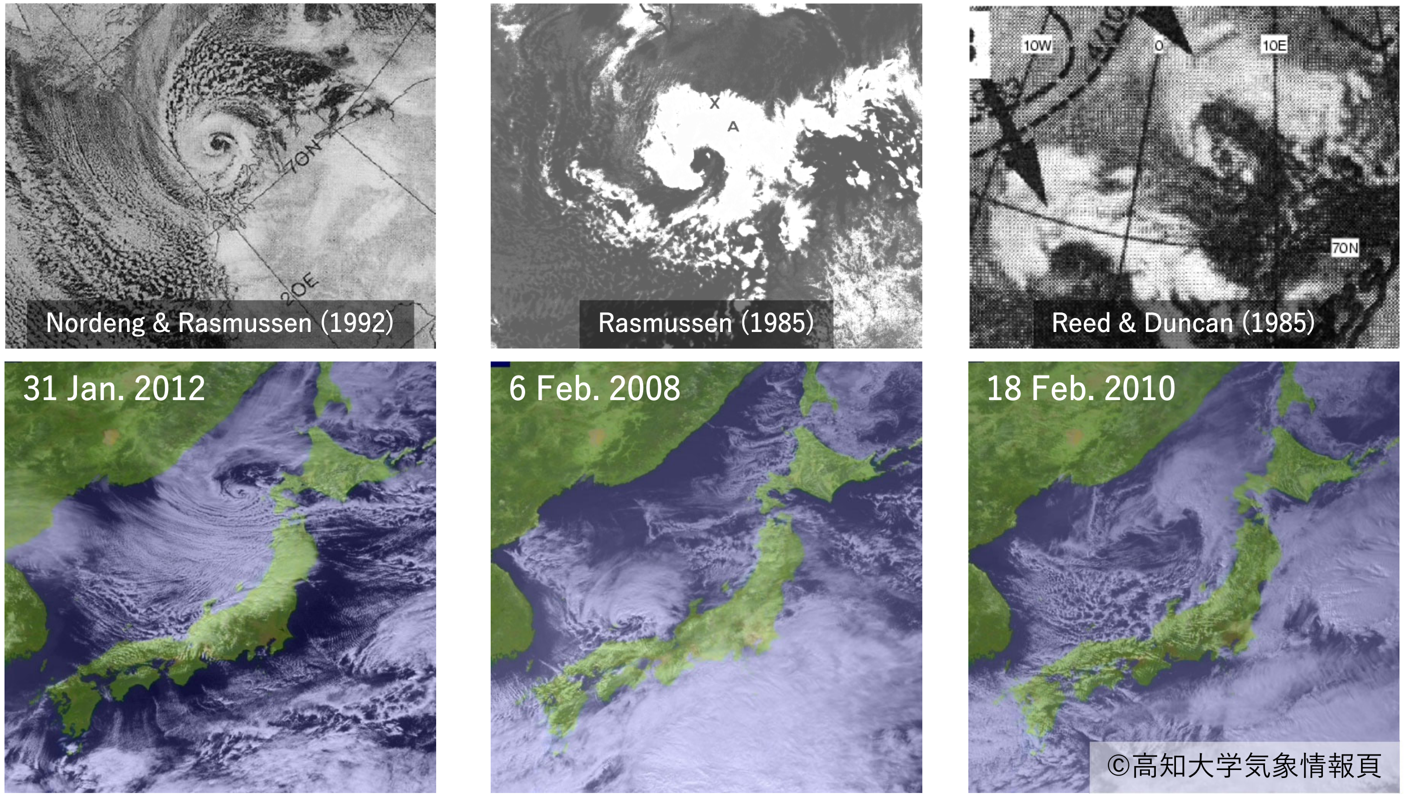

Nordic Seas

Sea of Japan

Spiral-shaped | Intermediate | Comma-shaped

Idealized experiments demonstrate that the dynamics of polar lows are continuous from TC-like to EC-like.

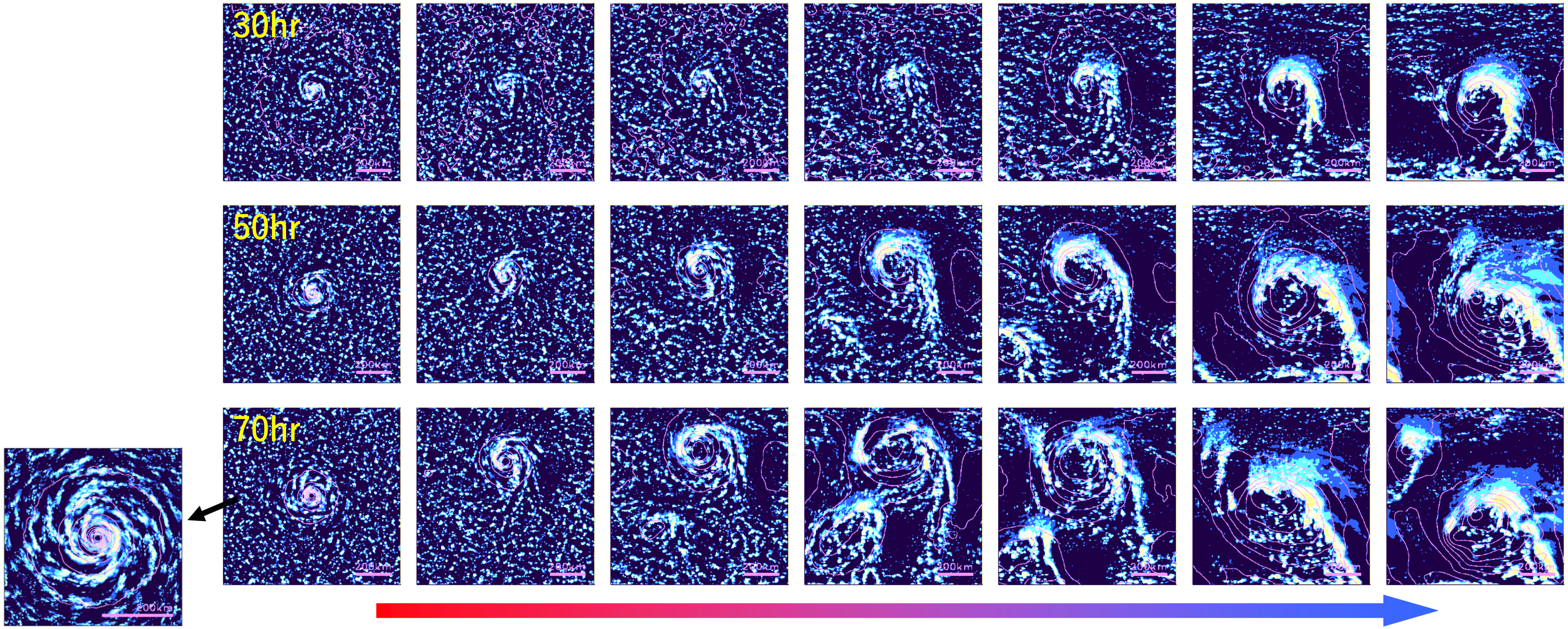

Higher-resolution
(5 km → 2km)

Weak Baroclinicity of environmental atmosphere*1 Strong

*1 Baroclinicity is maintained by spectral nudging.
In the real atmosphere, it can change during a life cycle.

Yanase and Niino (2005, 2007)

Similarly, idealized experiments on synoptic-scale cyclones demonstrate that there is no clear boundary between TCs and ECs.

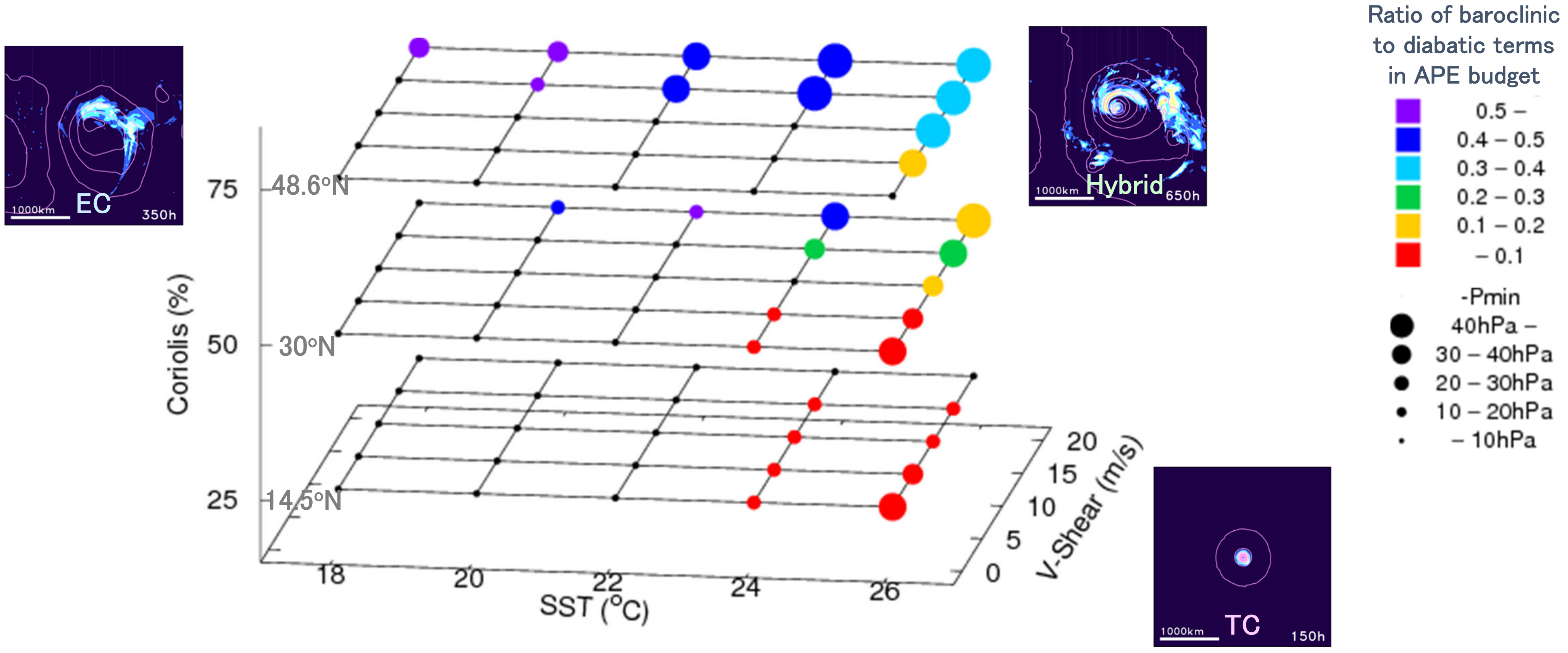

Yanase and Niino (2019)

Furthermore, a cyclone evolves from one type to another during its life cycle.

- Extratropical transition occur frequently in the western North Pacific and other regions.
- Tropical transition in the North Atlantic has been studied intensively.

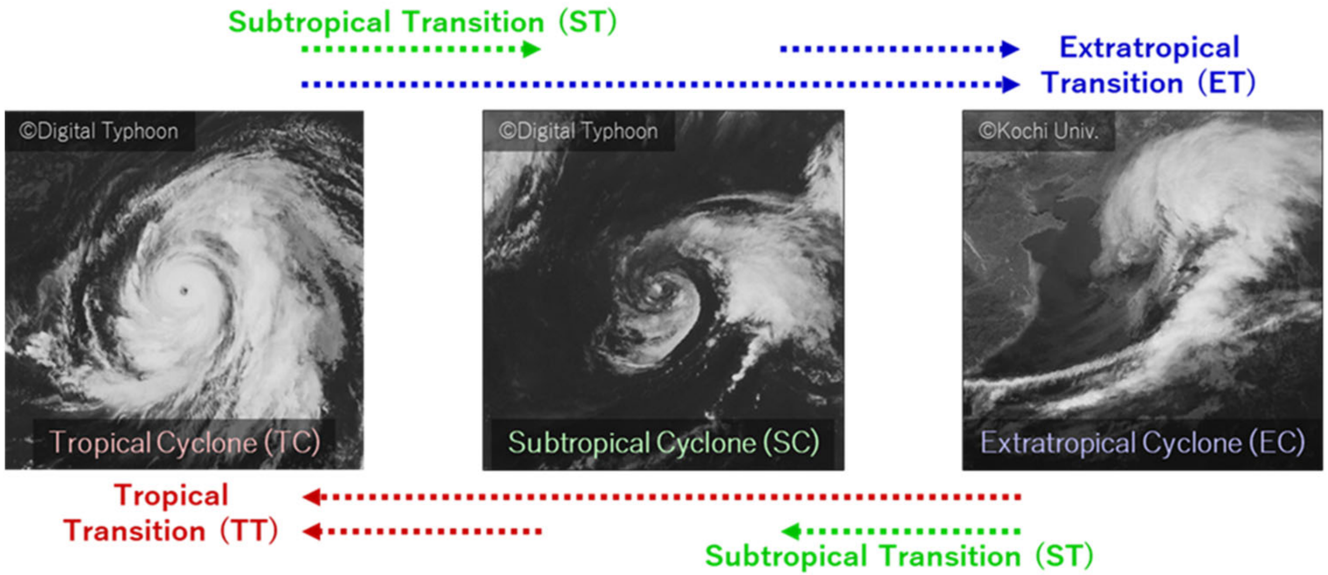

Subtropical cyclone
- ✓ Hybrid
- ✓ Synoptic-scale
- ✓ A cold core above a warm core

WMO ITWC-10 report, Wood et al. (2023)

[Summary]　1. Diversity of cyclones

- Various types of cyclones including hybrid cyclones form around the globe.
- Some cyclones show continuous change from one type to another.

2. Extratropical Transition (ET or ETT)

温帯低気圧化（温低化）

Typhoon Hagibis (2019) with torrential rain caused about 100 fatalities in Japan.
（令和元年東日本台風）

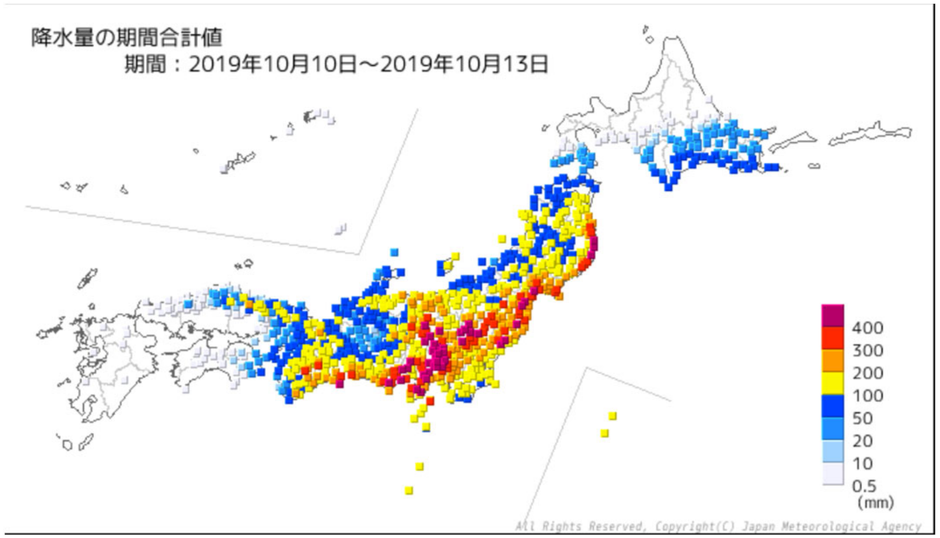

Total precipitation (mm)
accumulated from 10 to 13 October
気象庁 災害時気象報告

Shinkansen trains were flooded in Nagano
https://weathernews.jp/s/topics/202002/190135/

The torrential rain is attributed not only to a large amount of water vapor but also to frontal dynamics.

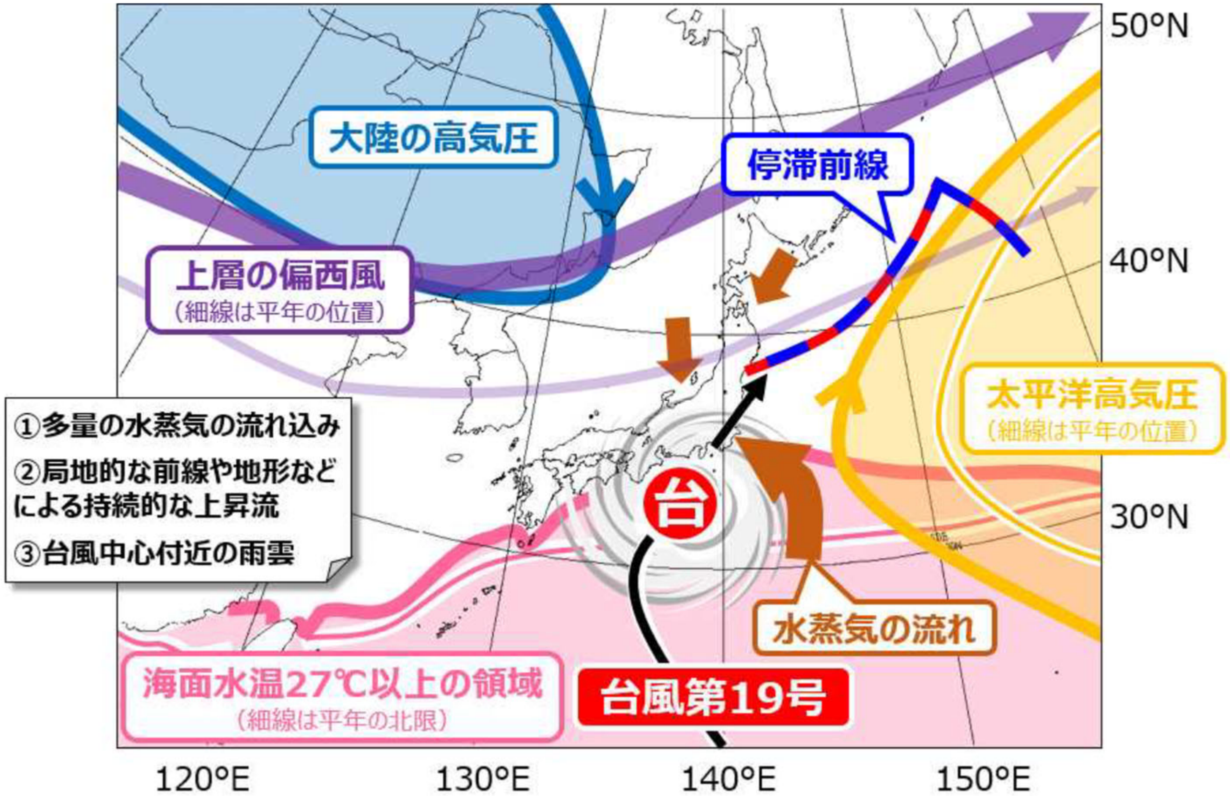

気象庁報道発表

Precipitation was concentrated to the left of the cyclone track.
(This characteristic has been observed in many ET cases)

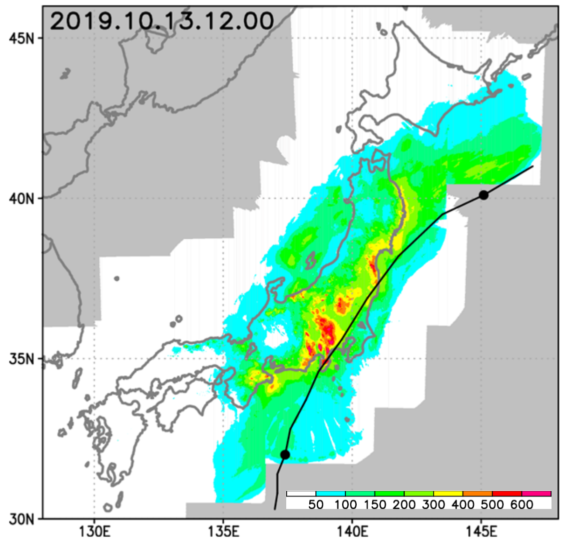

Radar/Raingauge-Analysis

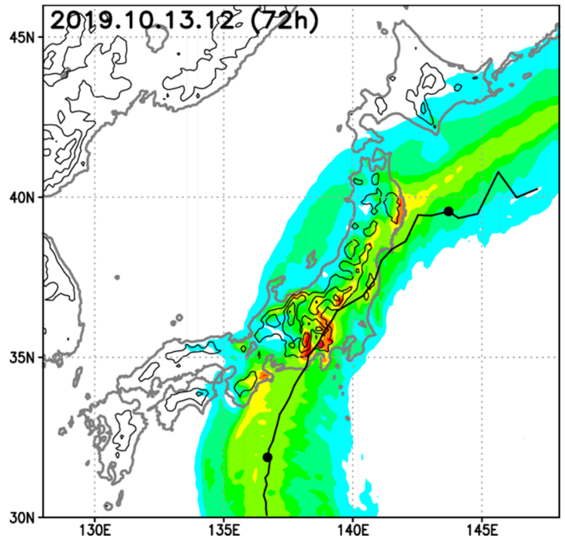

CTL experiment

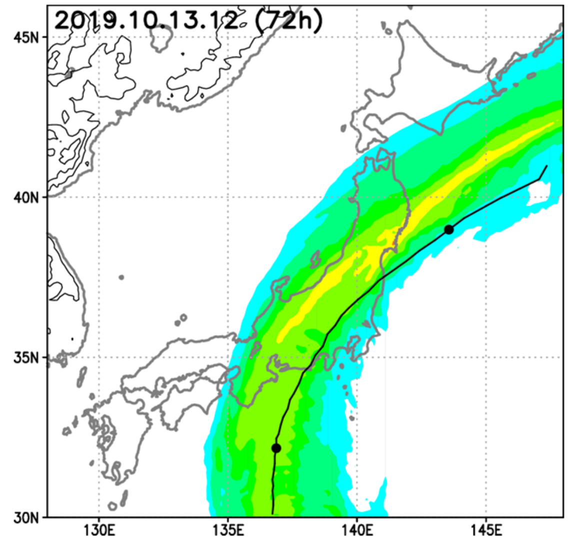

No topography/land experiment

Total precipitation (shading; mm) accumulated for 72 h from 1200 UTC 10 October
Track of Hagibis (black curves)
Ground elevation (contours every 500 m; middle and right panels)

Yanase et al. (2022)

The Japan Meteorological Agency (JMA) first classified Hagibis as an EC at 0300 UTC 13 October (T_E).

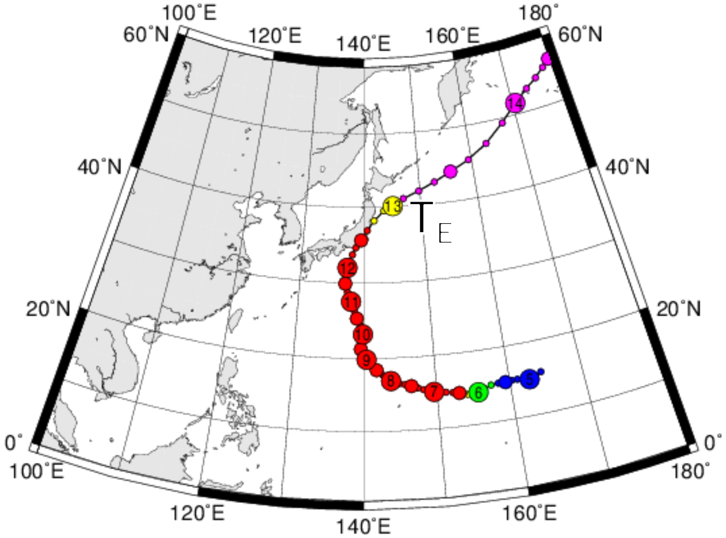

Track

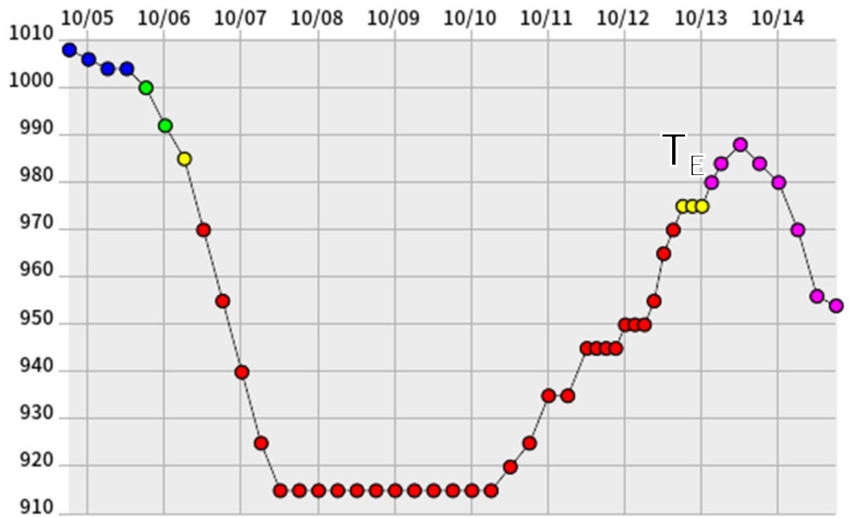

Minimum pressure

Magenta indicates that a cyclone was classified as an EC

The other colors denote the intensity of a cyclone. ©Digital Typhoon

Weather charts show that a frontal system existed near Hagibis before T_E.

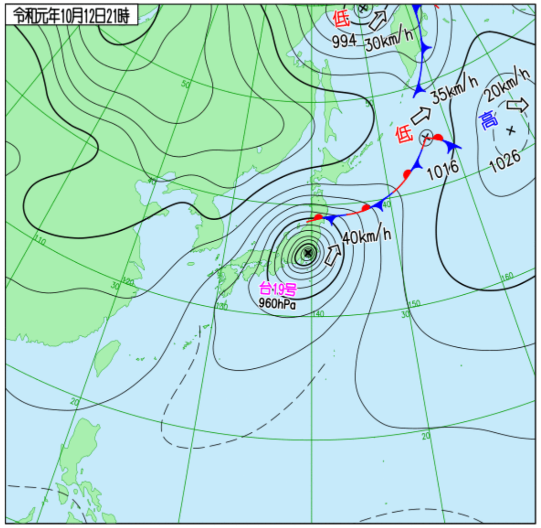

1200 UTC 12 Oct (T_E - 15 h)

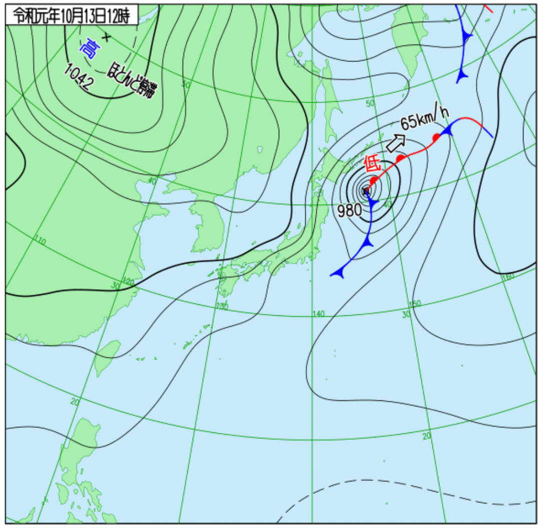

0300 UTC 13 Oct (T_E)

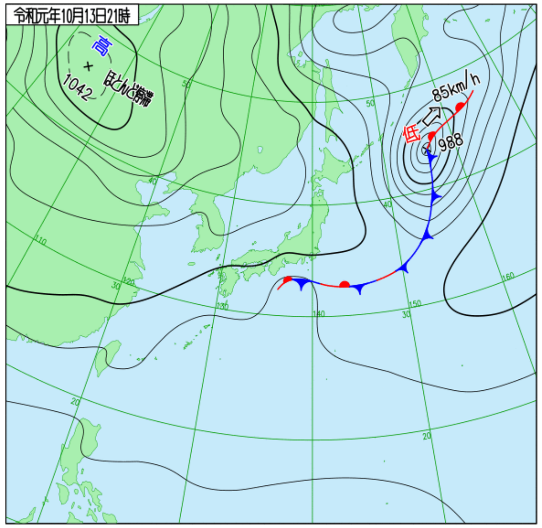

1200 UTC 13 Oct (T_E + 9 h)

Heavy precipitation was concentrated in the northern half of Hagibis 1~2 days prior to T_E.

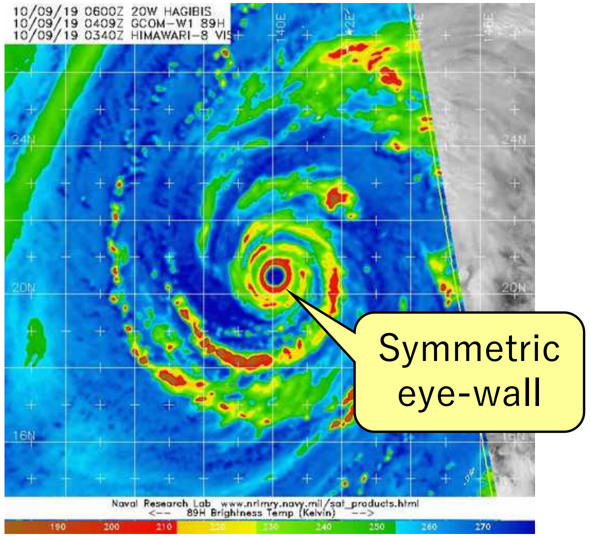

0400 UTC 9 Oct (T_E - 95 h)

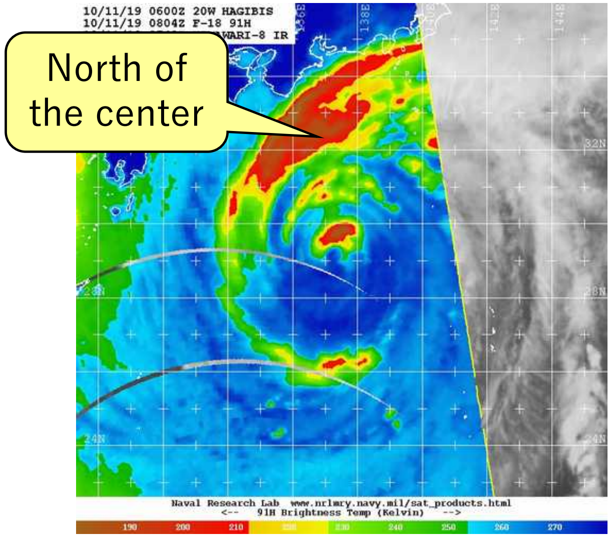

0800 UTC 11 Oct (T_E - 43 h)

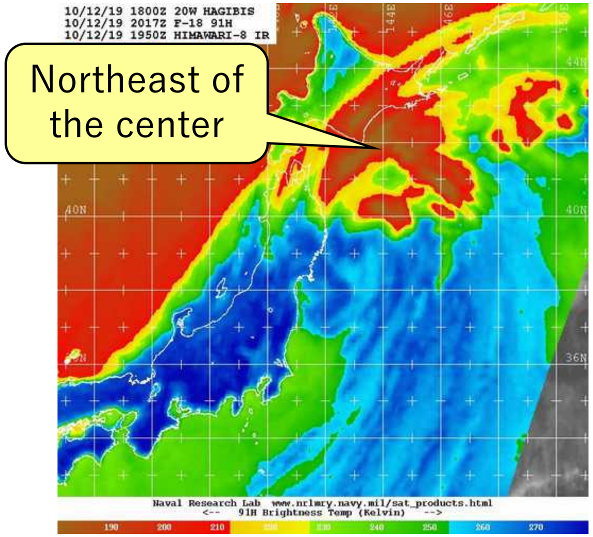

2000 UTC 12 Oct (T_E - 7 h)

Satellite microwave observation (85~91GHz, ice scattering)

As a TC gradually changes into an EC, ET has a beginning and an end.

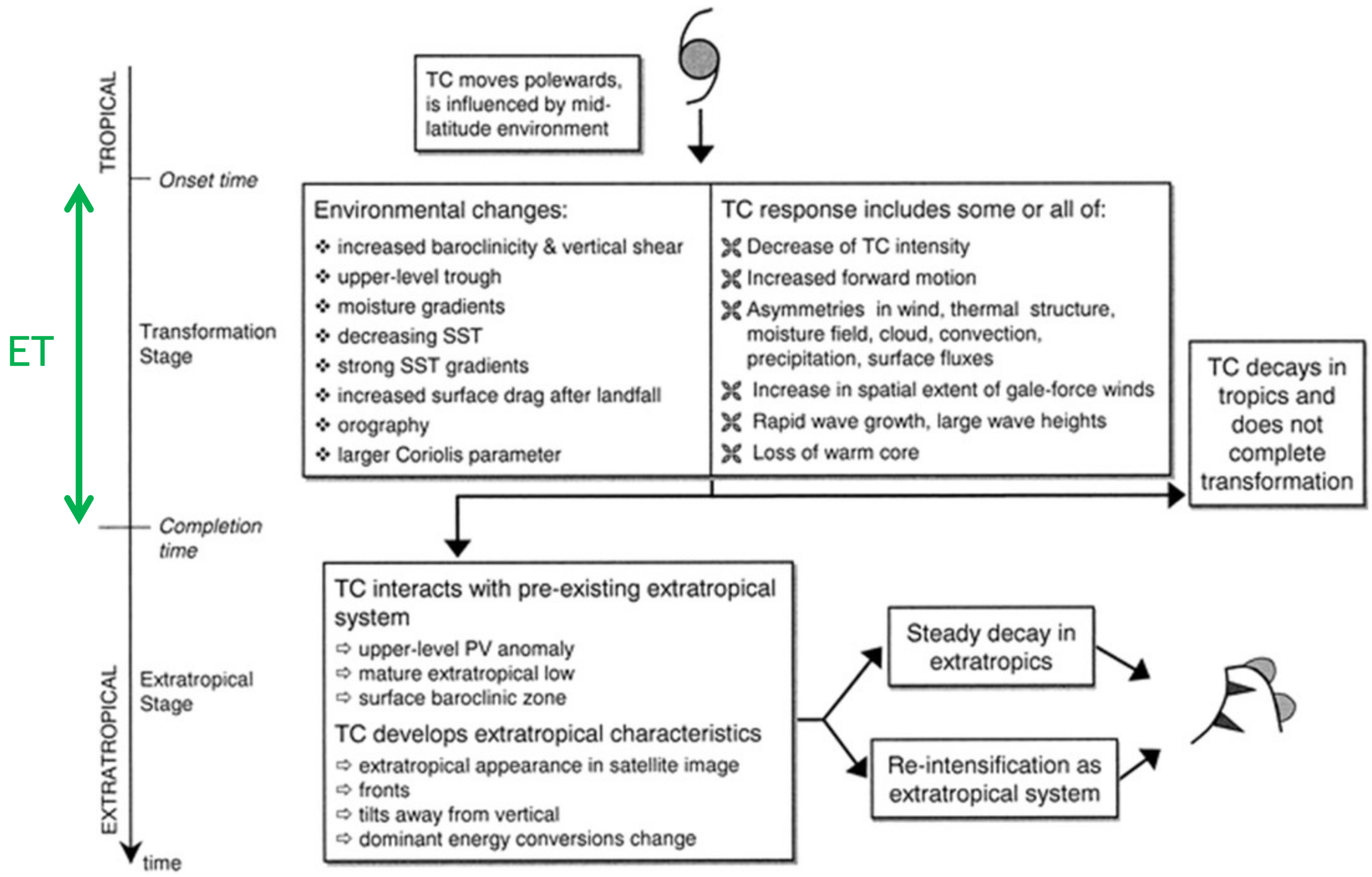

Jones et al. (2003)
Kitabatake (2006; in Japanese)

JMA analyzes an ET end based on three methods.

1. A front reaches the TC center in a weather map.
2. Geopotential height at 250 hPa is lower than thresholds. [A]
3. A total score based on 6 items exceeds a threshold (next slide).

Geopotential height at 250 hPa (shading)
and sea level pressure (contour)
in the JMA Global Spectral Model

Wood et al. (2023); Courtesy of JMA

The six items used for the score

i. Transition to SHEAR pattern
(vertical wind shear is increasing)

ii. Absence of dense cloud within 1.5° of the center
(convective cloud is suppressed)

iii. Absence of south-convex Ci or dense cloud bands southeast/southwest of the center.
(upper and lower circulation is out of alignment)

iv. Brightness temperature of -31°C or higher in the center in water vapor imagery
(no wetness resulting from upper-layer divergence)

v. SST is equal to or lower than 26°C or lower.

vi. SST is equal to or lower than 24°C or lower

Wood et al. (2023); Courtesy of JMA

JMA forecasts an ET end based on four methods.

- An objectively analyzed front[A] by the NWP model reaches the TC center.
- The Cyclone Phase Space diagram indicates “asymmetry” and “cold core structure”.
- SST is equal to or lower than 24/26°C or lower.
- Geopotential height at 250 hPa is lower than thresholds.

Thermal frontal parameter based on equivalent potential temperature at 925 hPa (shading) and sea level pressure (contour) in the JMA Global Spectral Model

Wood et al. (2023); Courtesy of JMA

Structures gradually change during ET.

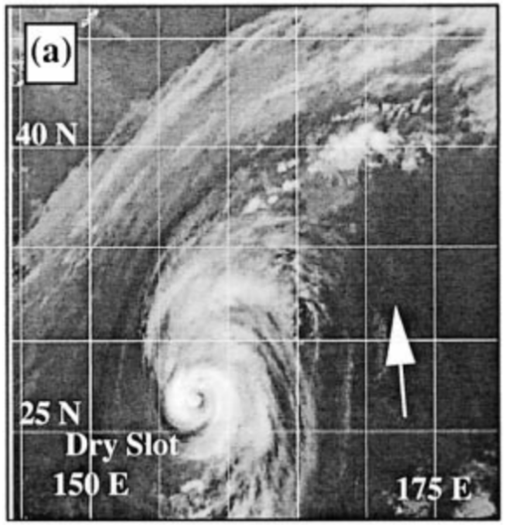

0332 UTC 28 Sep

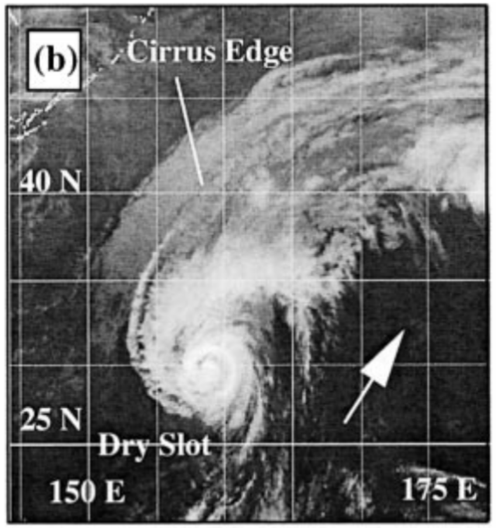

0032 UTC 29 Sep

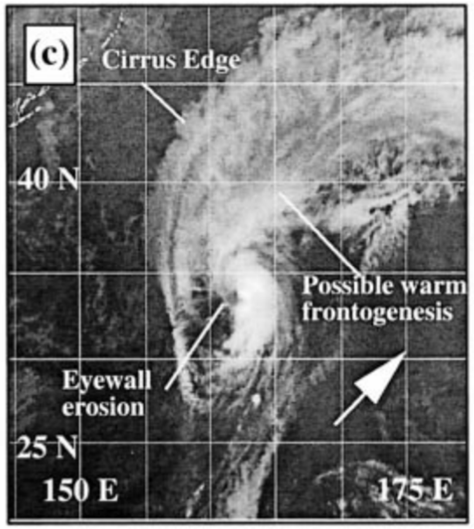

1232 UTC 29 Sep

IR imagery of Typhoon Ginger (1997)

Klein et al. (2000)

Structures gradually change during ET.
(conceptual model)

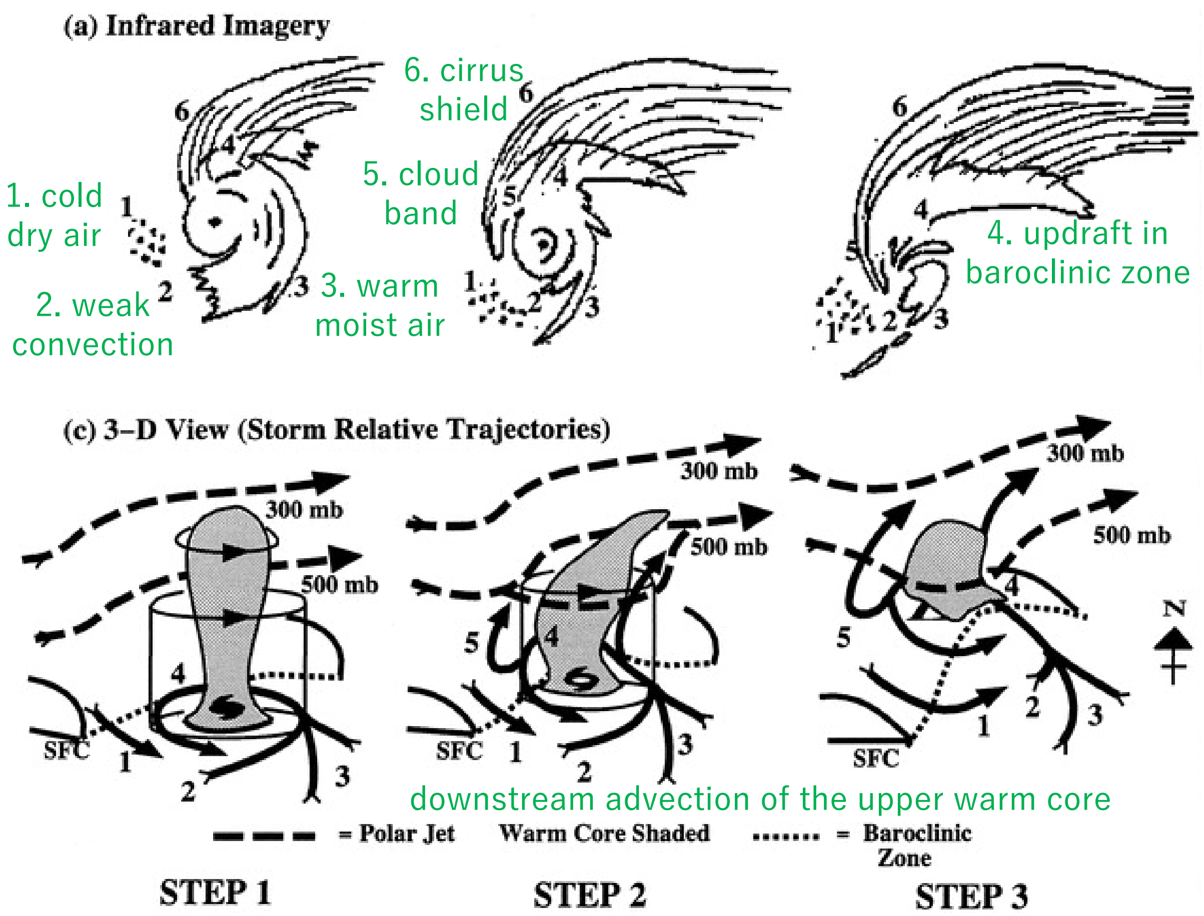

Klein et al. (2000)
Evans et al. (2017)

[Summary]　2. Extratropical transition

- ET has a beginning and an end.
- The ET end corresponds to the time when a cyclone is first classified as an EC.

3. Cyclone Phase Space (CPS)

低気圧相空間

Parameter B: cyclone thermal symmetry

$$B = h(\overline{Z_{600\ hPa} - Z_{900\ hPa}}|_R - \overline{Z_{600\ hPa} - Z_{900\ hPa}}|_L)$$

Z: geopotential height
h=+1/-1 for the Northern/Southern Hemisphere
R/L: a semicircle right/left of storm motion

900–600 hPa thickness (shading; m)
500 km radius (circle)
direction of motion (bisecting line)

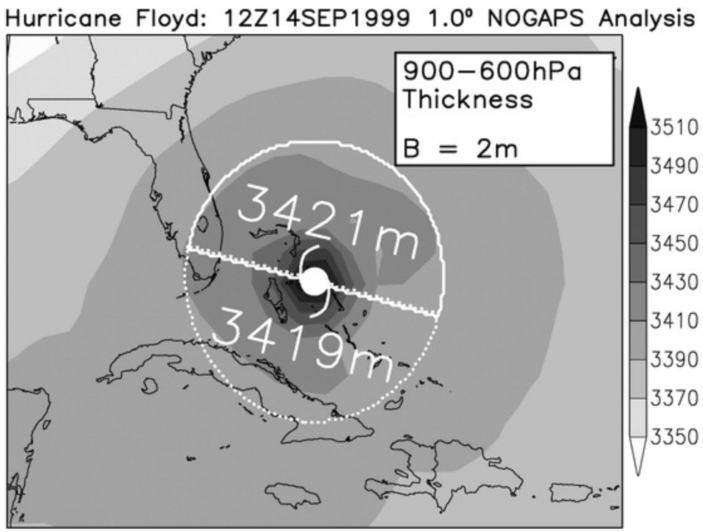

TC: symmetric (B<10)

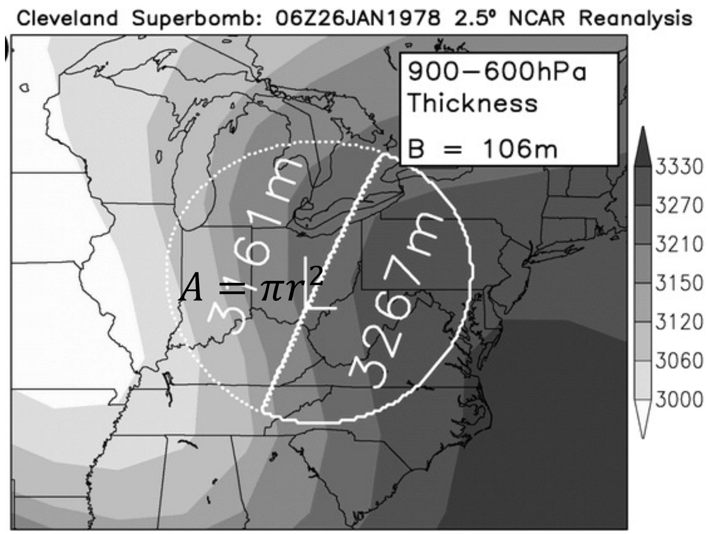

EC: asymmetric (B>10)

Hart (2003)

Parameters $-V_T^L$ & $-V_T^U$: cyclone warm/cold core

$$-V_T = \frac{\partial (Z_{MAX} - Z_{MIN})}{\partial \ln p}$$

$-V_T^L$: lower troposphere (900–600 hPa)

$-V_T^U$: upper troposphere (600–300 hPa)

Z_{MAX}/Z_{MIN}: A maximum/minimum of geopotential height within a radius of 500 km

[Left] zonal cross section
height (solid contour; every 2000 m)
height anomaly from zonal mean
(dotted contour; every 50 m)
[Right] vertical profile of Z_{MAX}-Z_{MIN}

A cold core does not necessarily mean a minimum temperature anomaly just above a surface cyclone center.

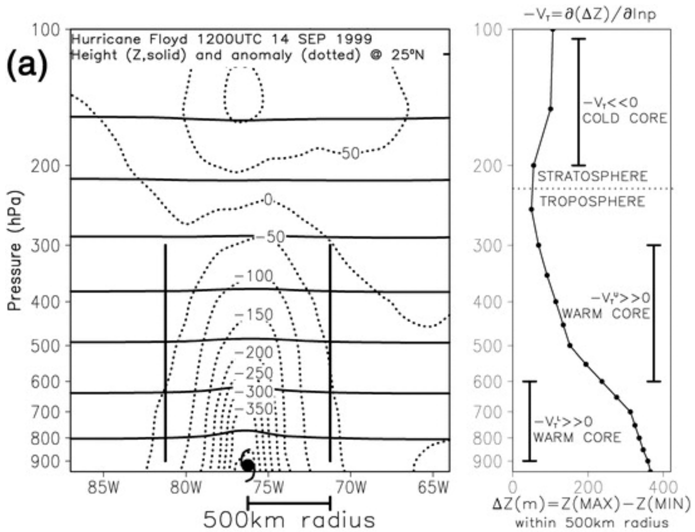

TC: warm core ($-V_T^L>0$, $-V_T^U>0$)

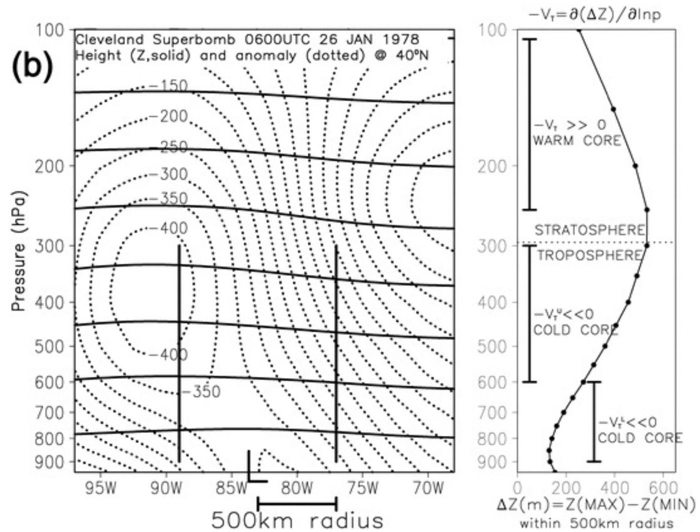

EC: cold core ($-V_T^L<0$, $-V_T^U<0$)

Hart (2003)

The continuous nature of cyclone structures and transitions is expressed in a three-parameter space (two diagrams).

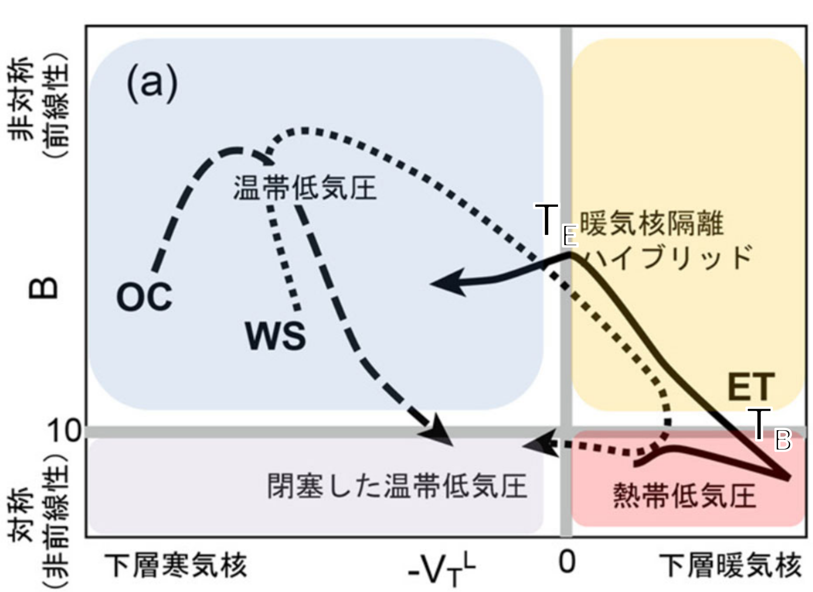

Diagram 1 ($-V_T^L$ vs. B)

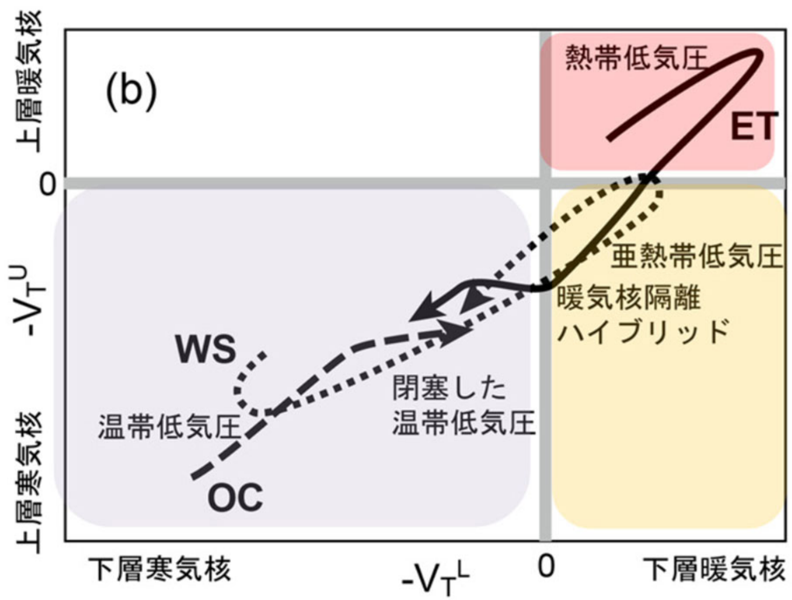

Diagram 2 ($-V_T^L$ vs. $-V_T^U$)

北畠 (2019) 総観気象学基礎編

ET of Typhoon Hagibis (2019): Diagram 1

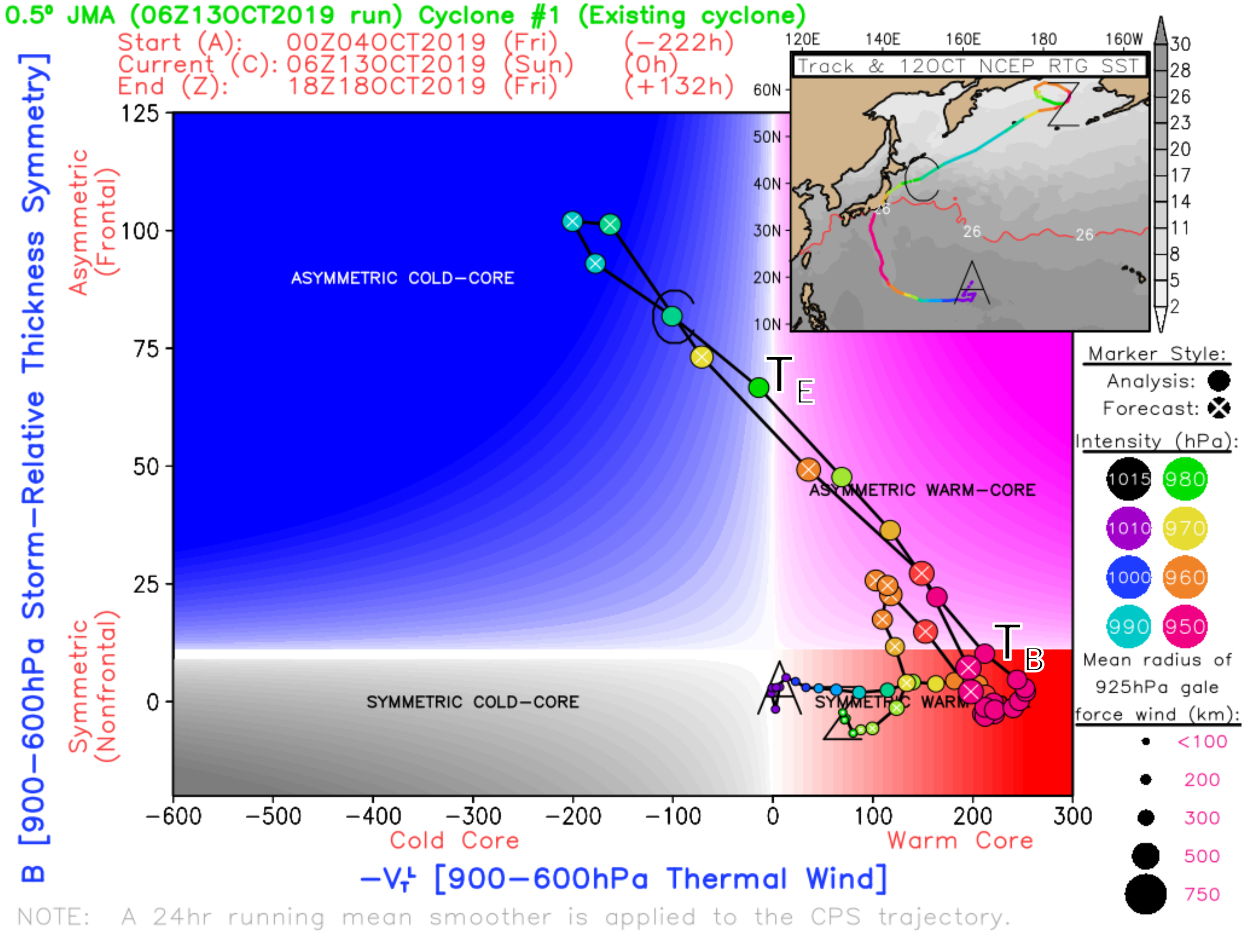

T_B: beginning of ET
T_E: end of ET

Website of cyclone phase evolution
https://moe.met.fsu.edu/cyclonephase/

ET of Typhoon Hagibis (2019): Diagram 2

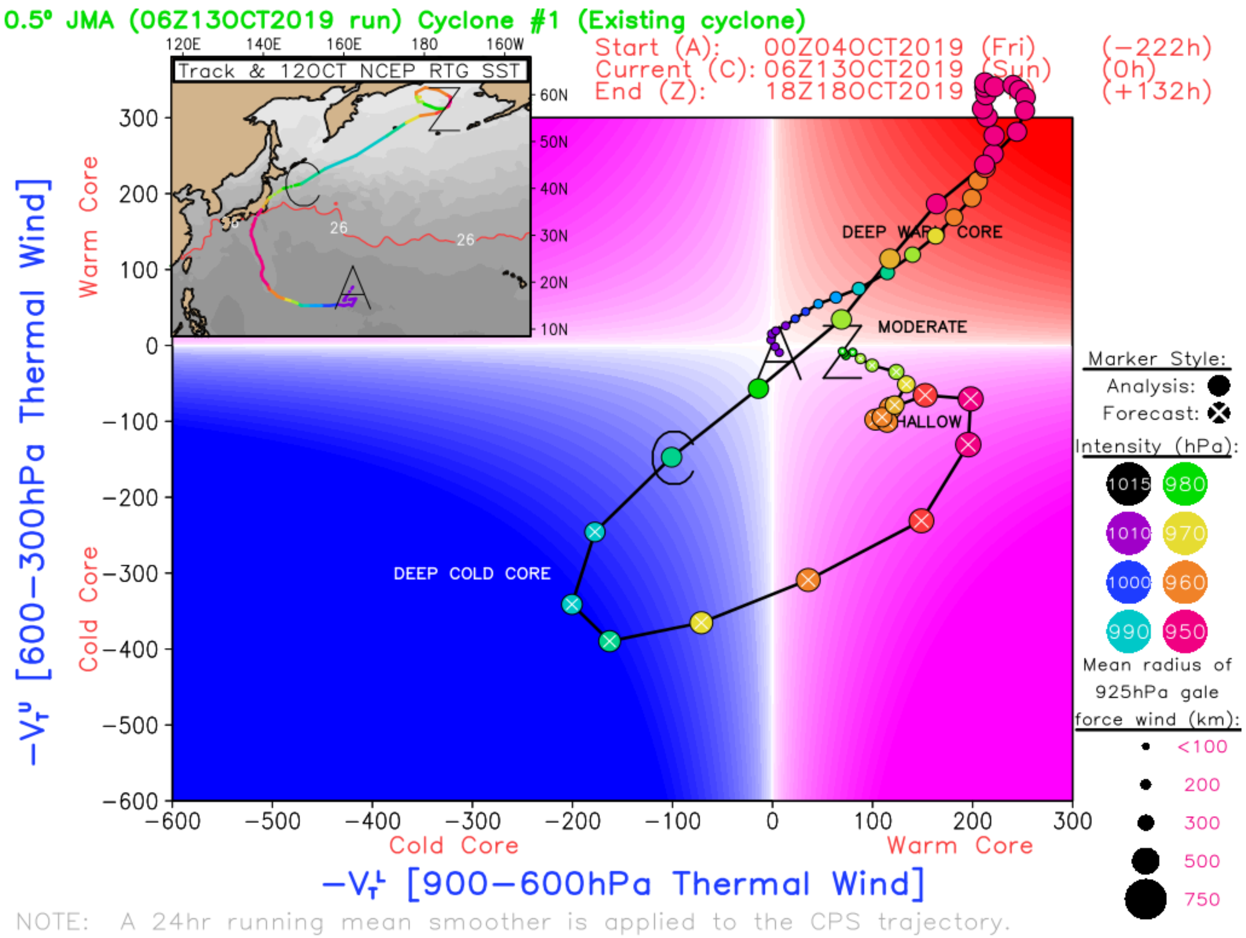

Website of cyclone phase evolution
https://moe.met.fsu.edu/cyclonephase/

The CPS is widely used as an objective cyclone classification method.

- The WMO 10th International Workshop on Tropical Cyclones (IWTC-10) summarized recent progress in research and operation.
- The working group on “phase transitions” reviewed many studies based on the CPS and discussed classification methods including the CPS and those developed in operational centers.

IWTC-10 in Bali in December 2022

Working group on “Phase Transitions”

[Rapporteur] K. Wood, W. Yanase

[Member] J. Beven, S. Camargo, J. Courtney, C. Fogarty, J. Fukuda, N. Kitabatake, M. Kucas, R. McTaggart-Cowan, M. Reboita, J. Riboldi

Wood et al. (2022, 2023)

The CPS can provide global climatology of ET on a uniform basis.

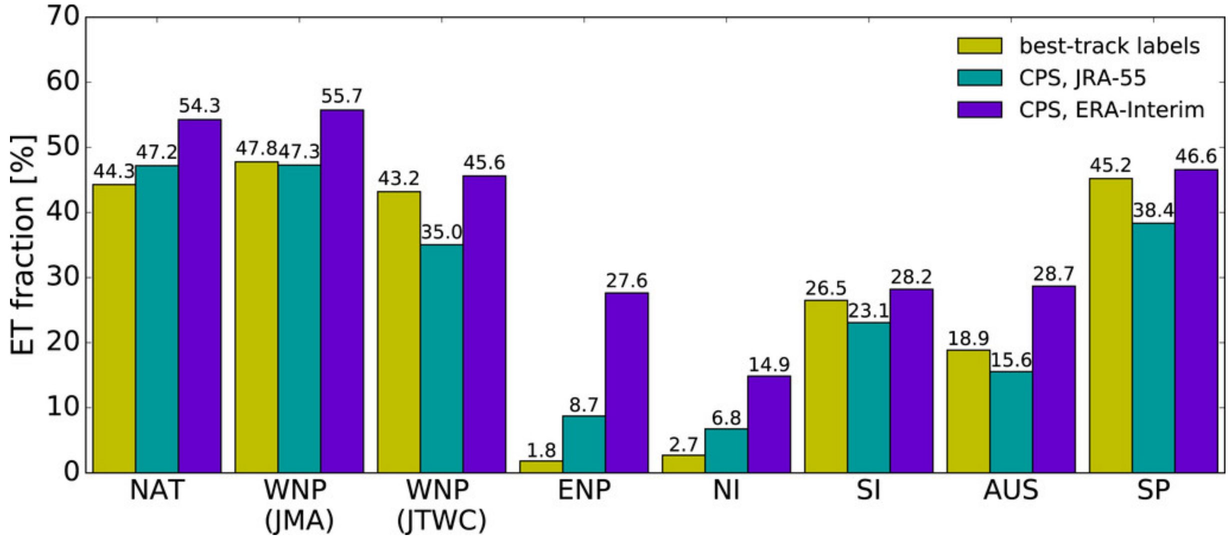

Bieli et al. (2019)

The CPS can classify subtropical cyclones objectively.

- Tropical storm Kirogi had an EC-like structure around its genesis time on 6 August 2012.
- The CPS indicates that a subtropical cyclone (SC) transitioned into a TC (tropical transition)

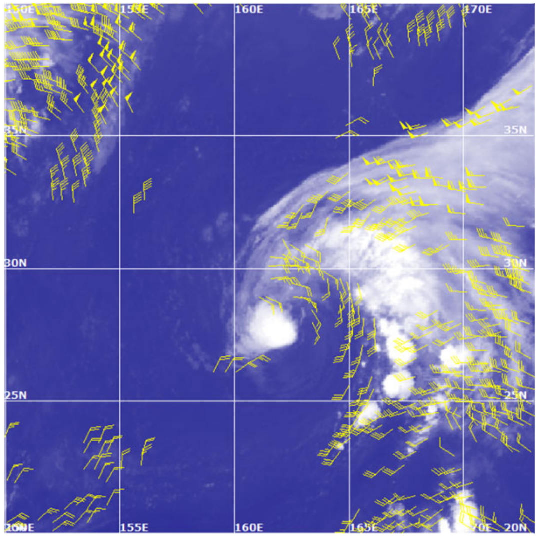

1200 UTC 6 Aug
(genesis, SC)

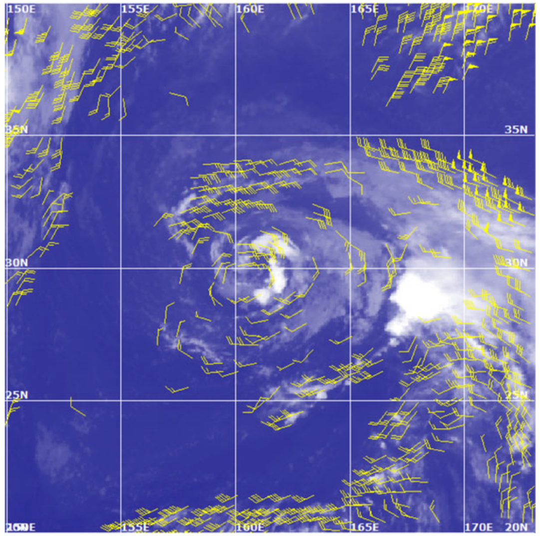

1200 UTC 7 Aug
(TC)

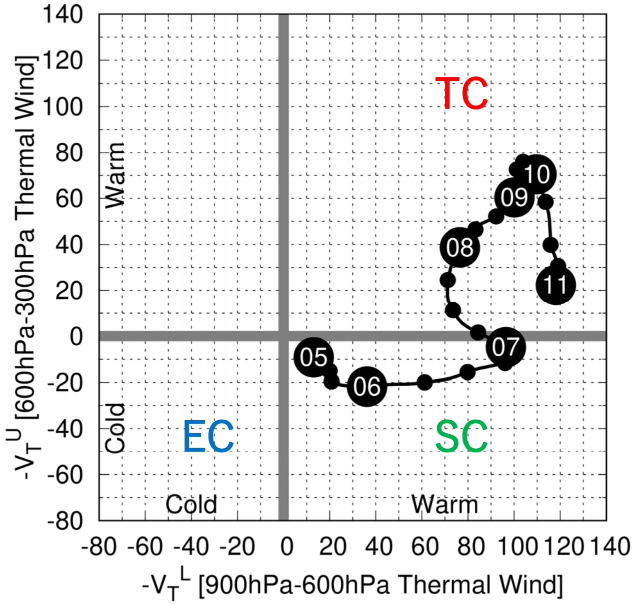

CPS analysis applied to a simulation

Yanase et al. (2023)

The CPS can explore the global distribution of different types of cyclones.

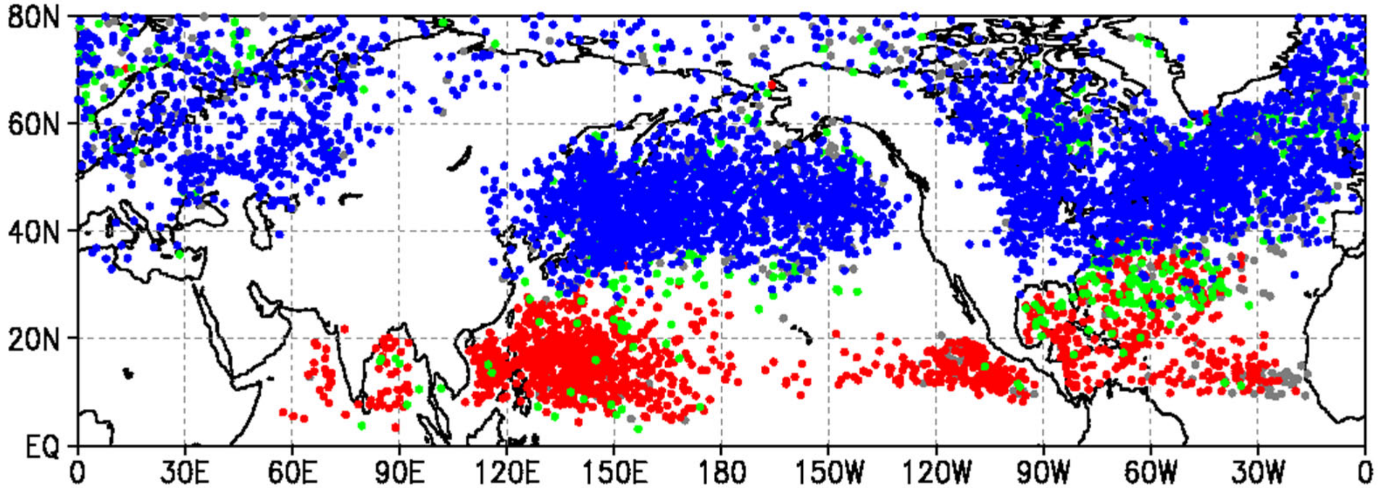

Climatology of different types of developing cyclones.
TC (red), EC (blue), Hybrid or SC? (green)
The CPS is applied to the JRA-25 reanalysis.

Yanase et al. (2014)

[Summary]　3. Cyclone Phase Space

- The CPS expresses the continuous nature of types and transitions of synoptic-scale cyclones.
- The CPS has been widely used as an objective cyclone classification method.

➔ Prof. Hart will give details in the lecture this afternoon.

4. ET around Japan

日本周辺の温低化

Typhoon Tokage (2004) with torrential rain caused 98 fatalities.

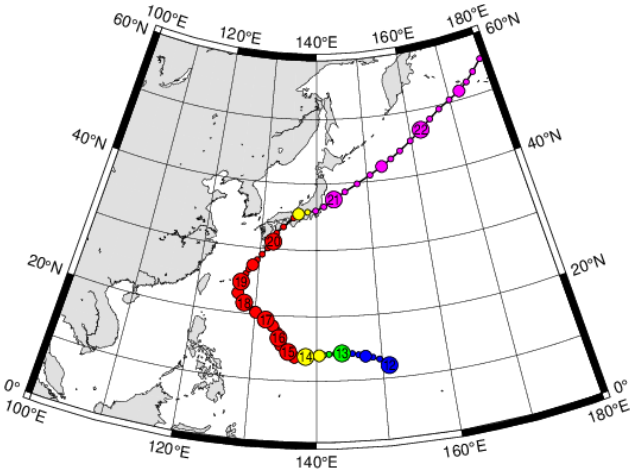

Track

Digital Typhoon

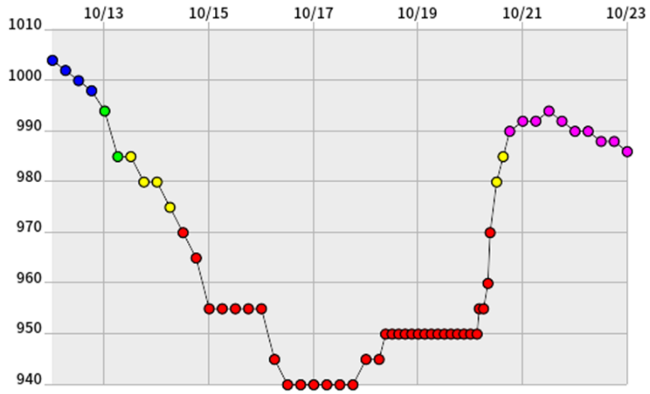

Minimum pressure

Digital Typhoon

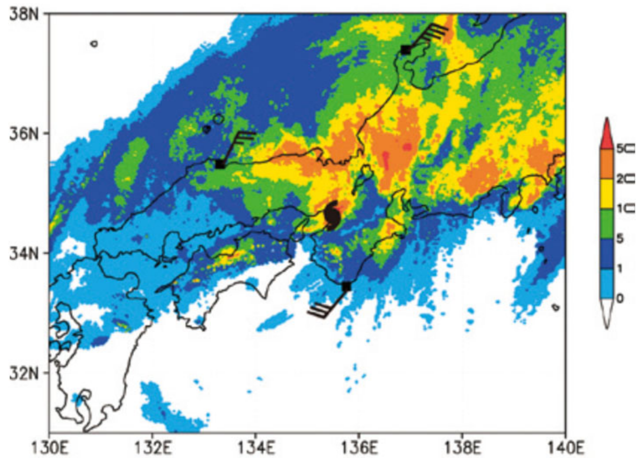

Radar/Raingauge-Analysis
0900 UTC 20 Oct. 2004

Kitabatake (2008)

Typhoon Marie (1954) caused 1361 fatalities including a ferry sinking.

(洞爺丸台風)

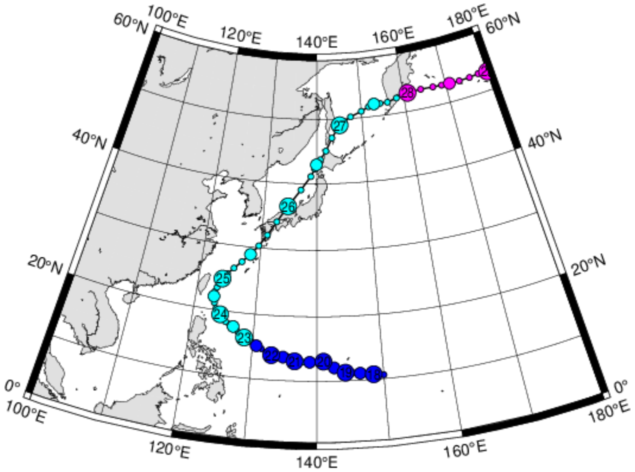

Track

Digital Typhoon

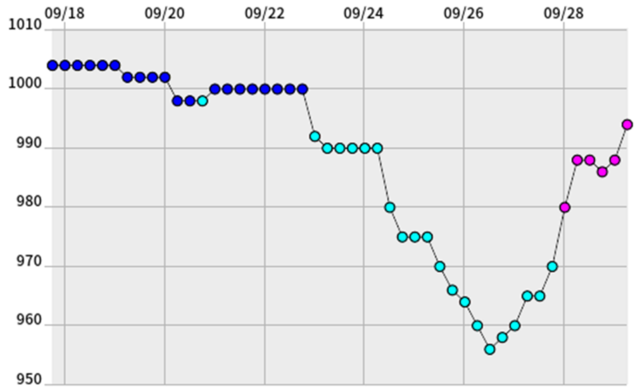

Minimum pressure

Digital Typhoon

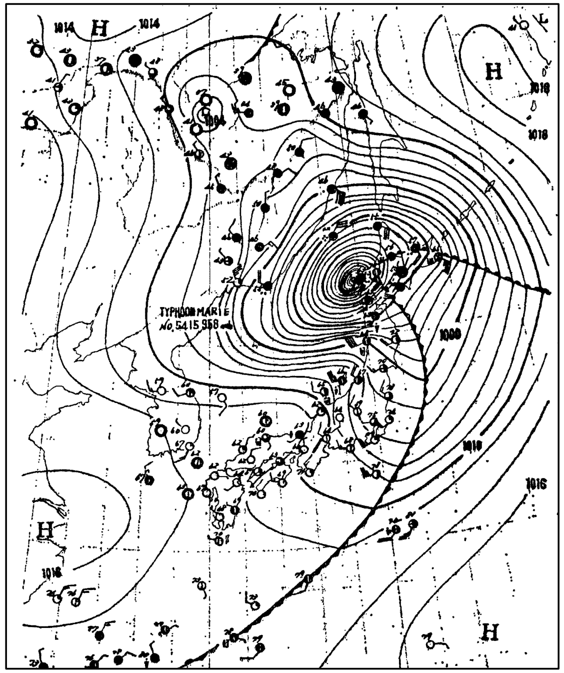

Weather chart

1200 UTC 26 Sep. 1954

村松 (1983)

Most of the poleward moving TCs complete ET after recurvature.

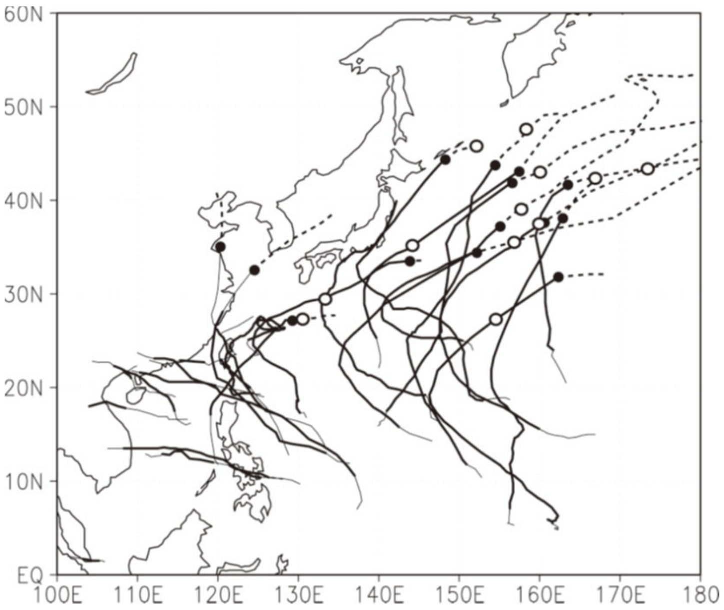

Tracks of 26 TCs in 2001
TC >34 kt (thick solid), TC <34 kt (thin solid), EC (dotted) in the JMA best track
ET end based on the JMA best track (closed circles)
ET end based on the CPS applied to the JRA-25 reanalysis (open circles)

Kitabatake (2011)

The transition period is 16.9 h on average.

Climatology of ET (1979-2004)
In the western North Pacific.
The CPS analysis is applied to
the JRA-25 reanalysis.

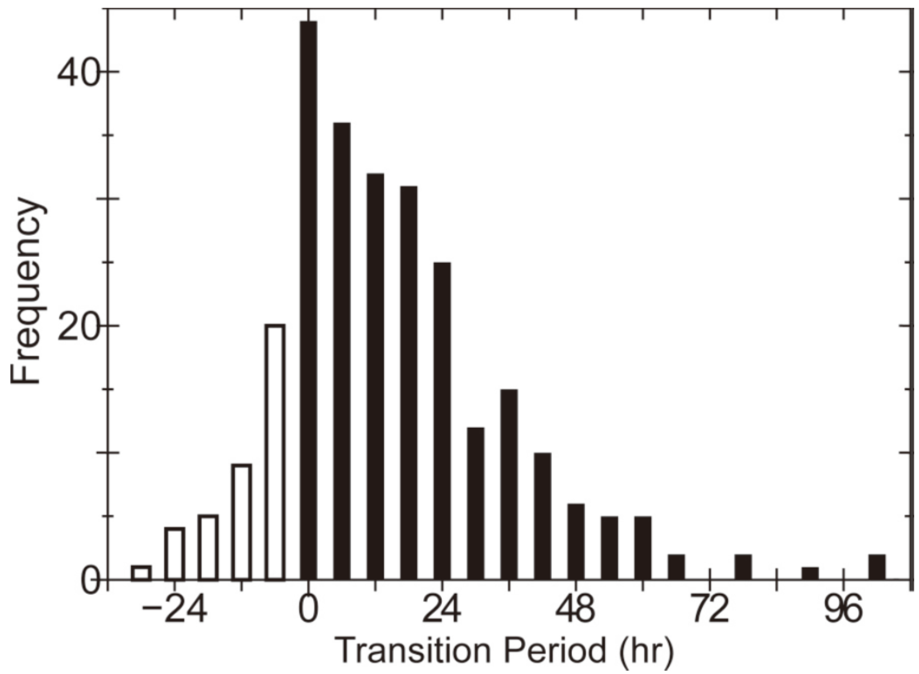

Frequency of the transition period (T_E-T_B).

Kitabatake (2011)

The ET season (Sep.) is later than the TC season (Aug.).

The ratio of ET to all TC reached ~60 % in Sep-Oct.

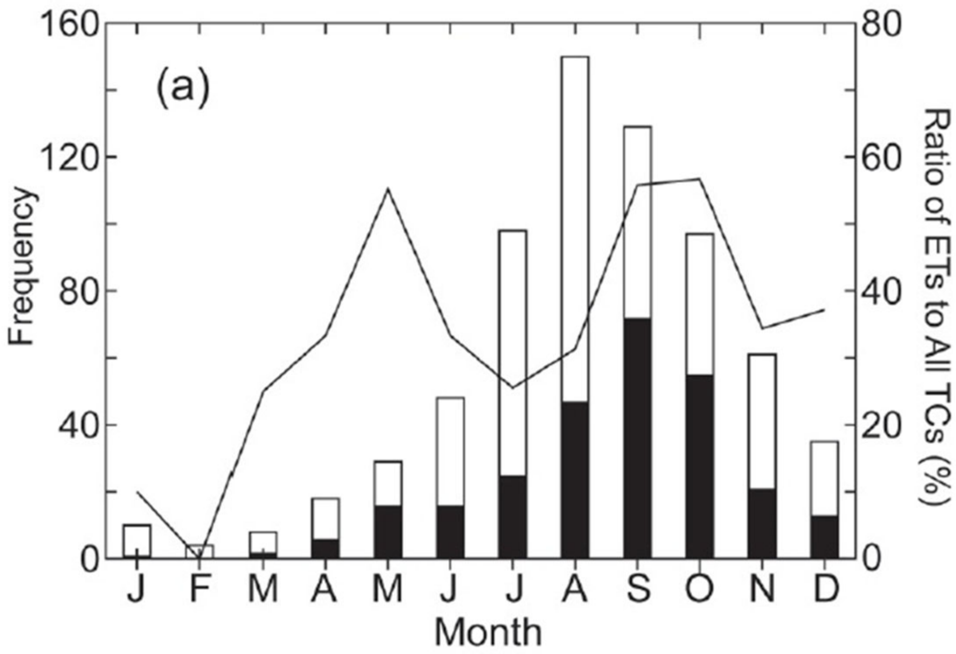

Frequency of ET(black bars) and all TC (white bars)
Ratio of ET to all TCs (solid line)

Kitabatake (2011)

The baroclinicity at the mid-latitudes is responsible for the higher ET ratio in autumn than in summer.

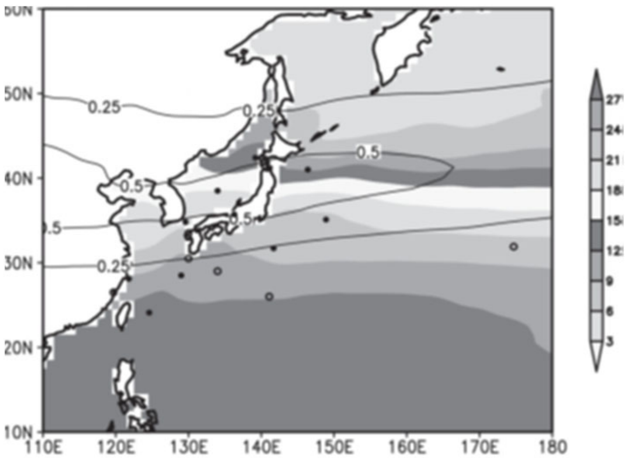

June

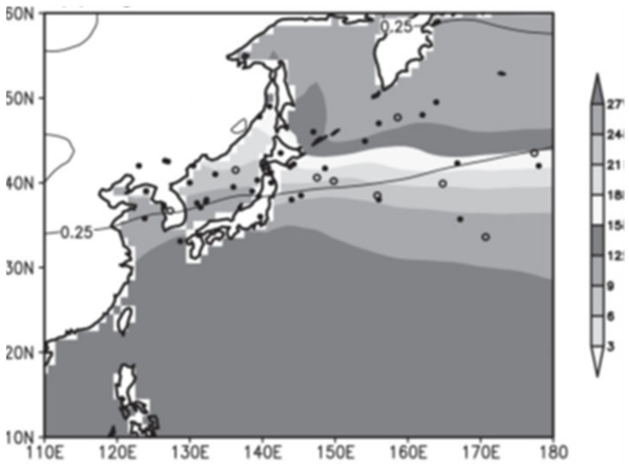

August

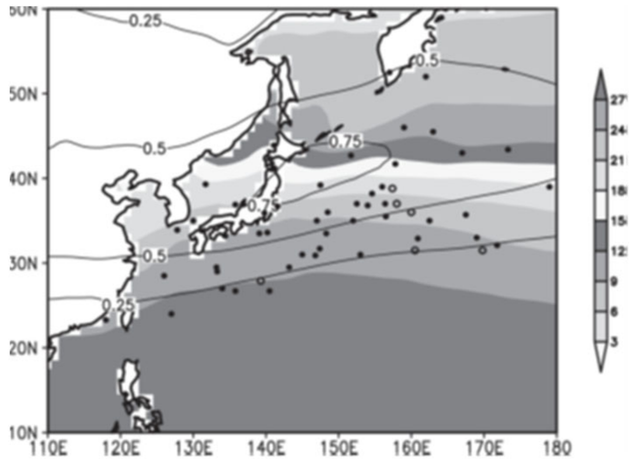

October

Locations of ET end (circles)
Eady growth rate (contour; every 0.25 day^{-1})
Sea surface temperature (shading; °C)

Kitabatake (2011)

[Summary] 4. ET around Japan

- TCs during ET have caused disasters in a different manner from TCs in the tropics.
- The ET season is later than the TC season because of larger baroclinicity in autumn.

5. Cyclone structures during ET

温低化中の低気圧構造

Cyclone structures including precipitation and surface wind during ET are different from those of typical TCs and ECs.

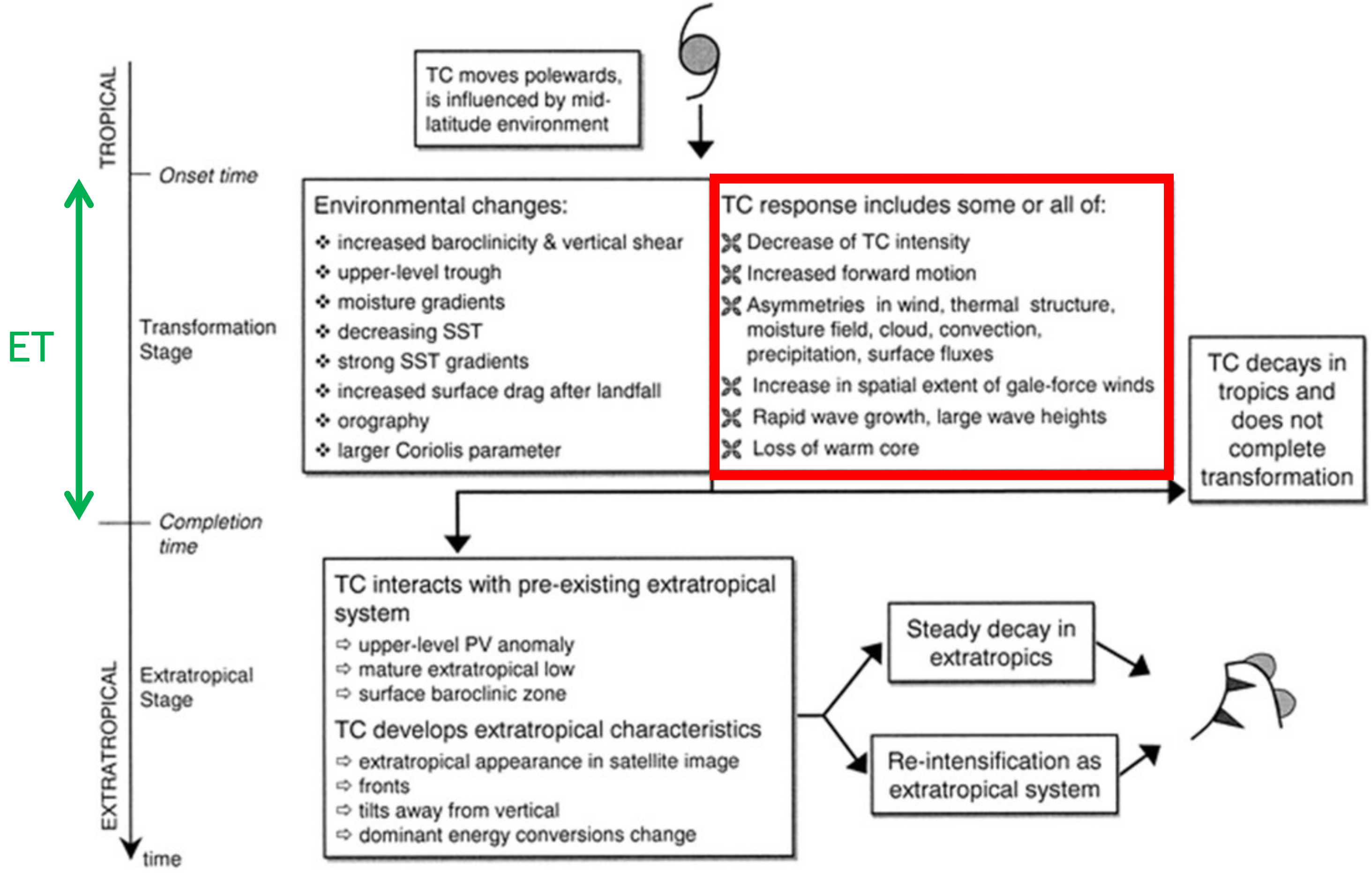

Jones et al. (2003)
Kitabatake (2006; in Japanese)

Precipitation is concentrated to the left of track during ET.

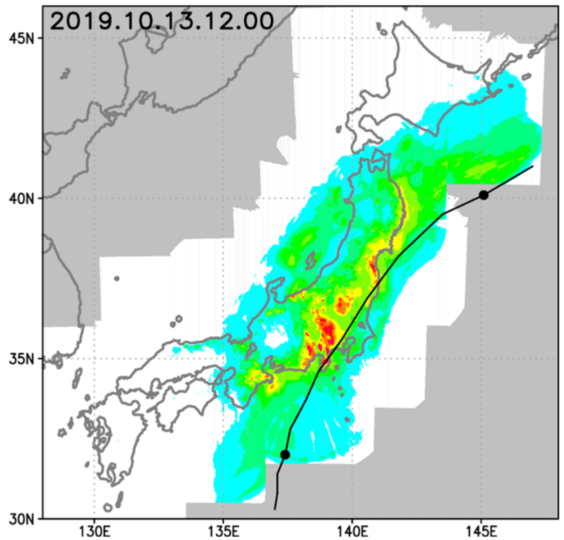

Typhoon Hagibis (2019)

Yanase et al. (2022)

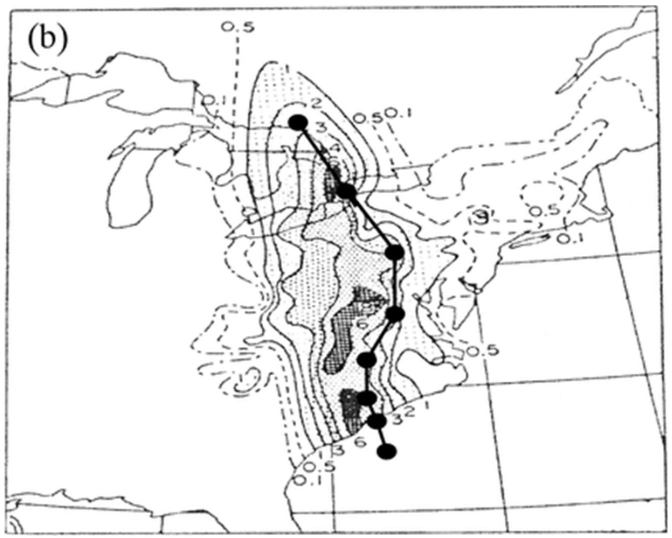

Hurricane Hazel (1954)

Palmén (1958), Jones et al. (2003)

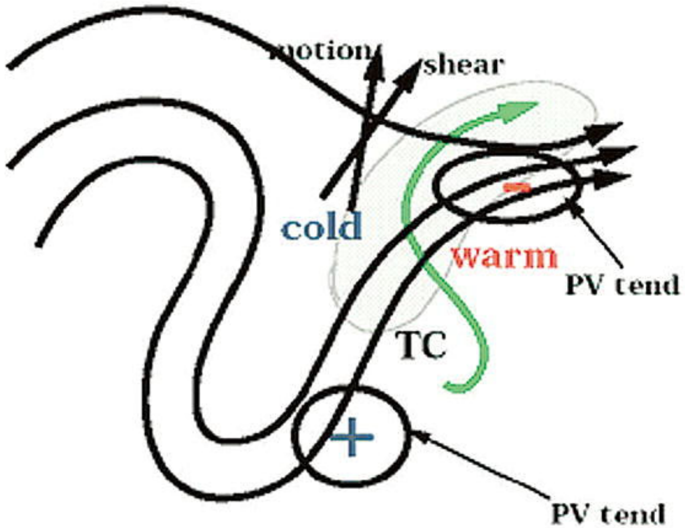

Conceptual model

Atallah et al. (2007)

[Other references] Deng and Ritchie (2018), Galarneau et al. (2013), Kitabatake (2008)

A warm front is enhanced during ET.

Typhoon Higos (2002)
during ET

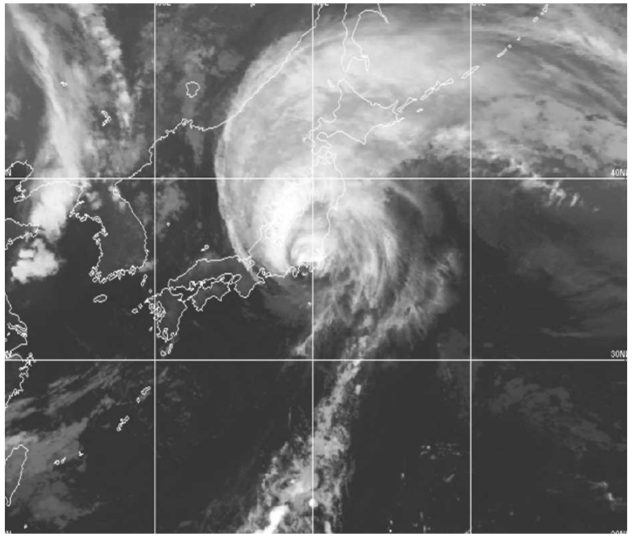

IR imagery at 1046 UTC 1 Oct.

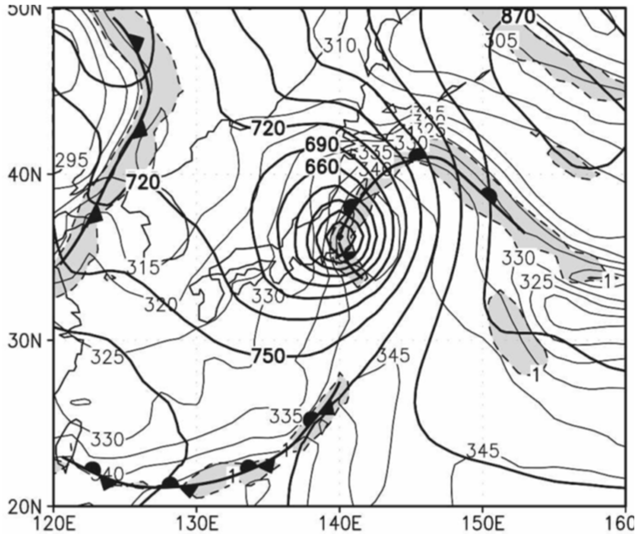

925 hPa surface at 1200 UTC 1 Oct.
Geopotential height
(thick contour; every 30 m)
Equivalent potential temperature
(thin contour; every 5 K)
Thermal frontal parameter
(> 1 K (100 km)$^{-2}$; shading)

[Other references] Colle et al. (2003), Harr and Elsberry (2000), Jones et al. (2003), Klein et al. (2000), Quinting et al. (2014)

Kitabatake (2008)

Delta-shaped precipitation pattern during ET.

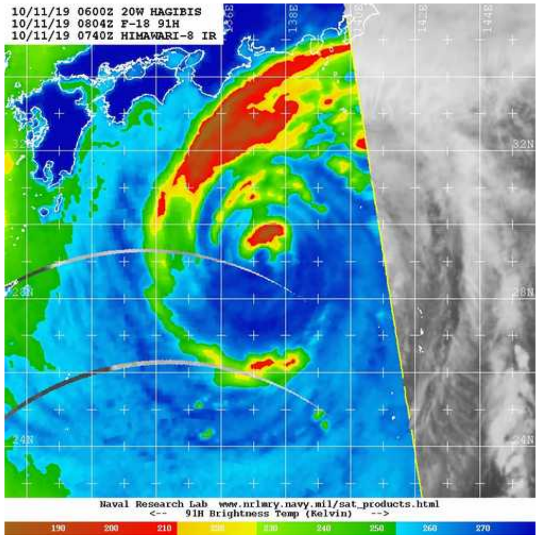

Typhoon Hagibis (2019)

Yanase et al. (2022)

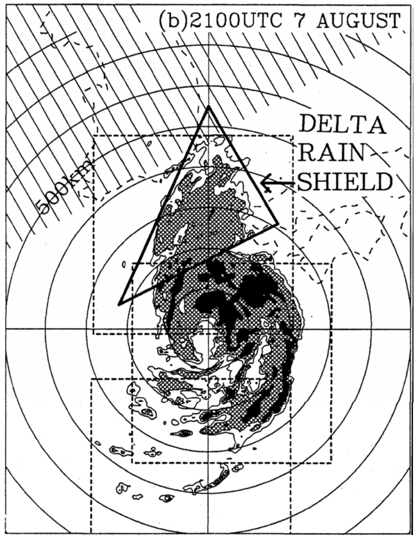

Radar echoes of T9210

Shimazu (1998)

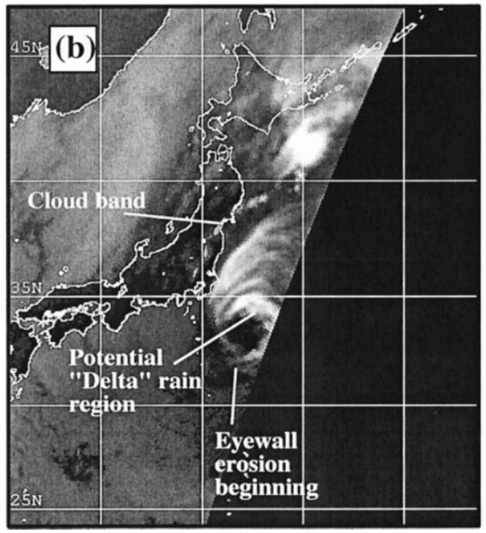

85 GHz SSM/I image of Typhoon David (1997)

Klein et al. (2000)

[Other references] Harr and Elsberry (2000), Kitabatake (2002), Ritchie and Elsberry (2001)

The area of intense wind increases during ET.

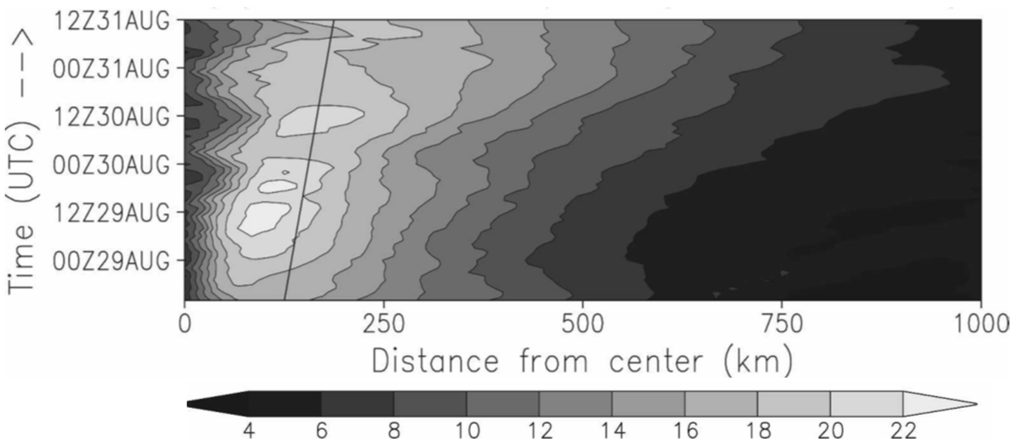

Hurricane Bonnie (1998)

10 m wind speed

Evans and Hart (2008)

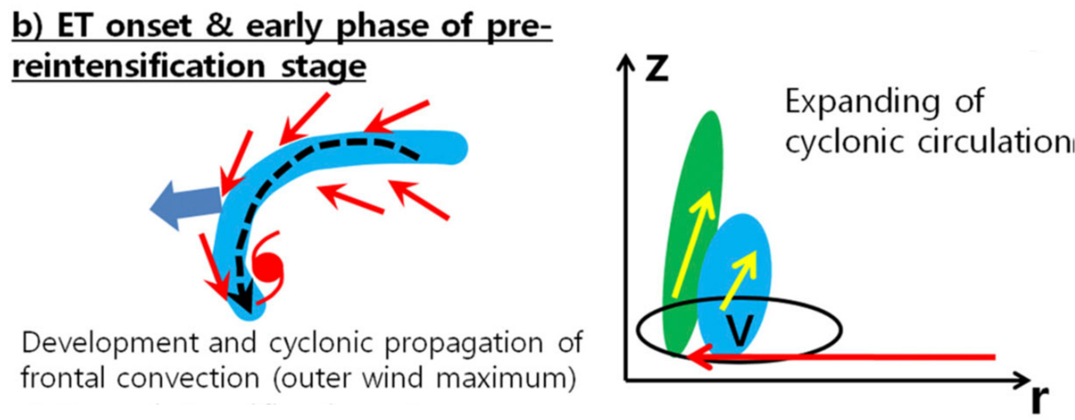

Conceptual model

Local wind maximum (black)
PBL inflow (red)
Eye-wall convection (green)
Frontal convection (blue)

Shin et al. (2019)

Surface wind is strong not only right of track but also left of track during ET (horseshoe-shaped pattern).

Classification of surface wind fields associated with landfall TCs over Japan from 1979 to 2014

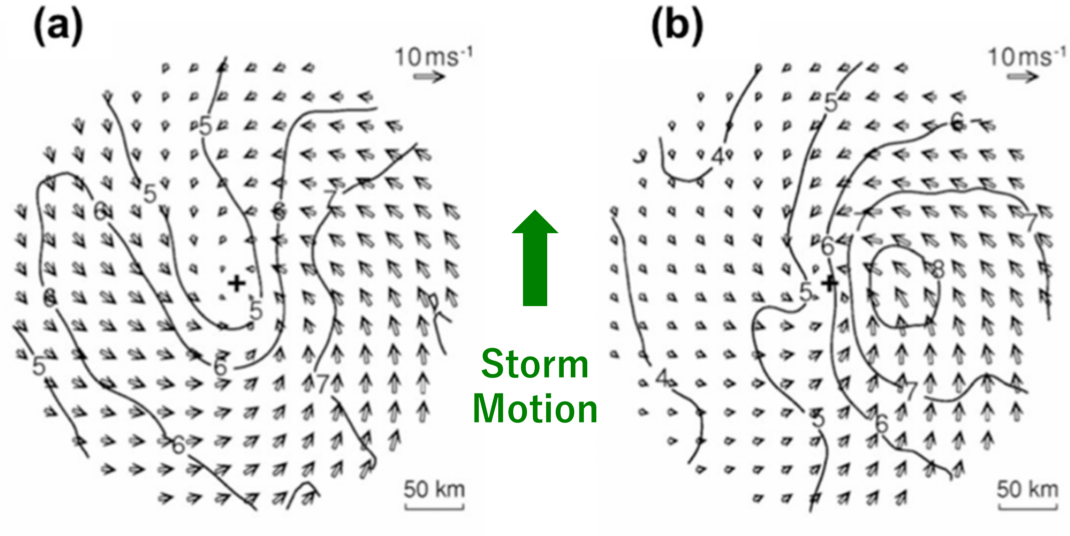

Horseshoe-shaped class (linked to ET)

All classes

Fujibe and Kitabatake (2008)
Kitabatake and Fujibe (2009)
Evans et al. (2017)

ET processes also show variation due to synoptic-scale conditions such as upper-level mobile troughs and preexisting fronts.

[Left] IR imagery

[Middle]
PV at 300–200 hPa (shading)
Geopotential height at 250 hPa (dashed contour)
Lower tropospheric front

[Right] Zonal cross section
PV (shading)
Potential temperature (dashed contour)

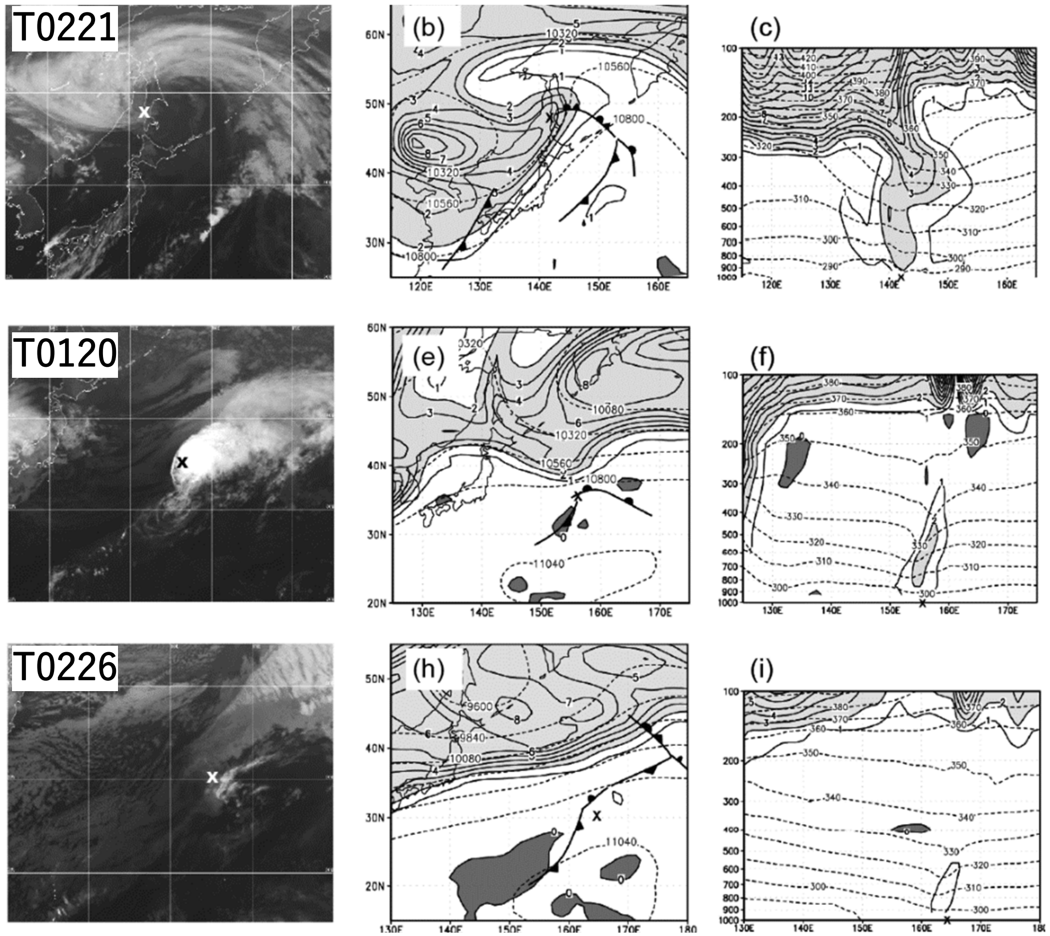

Kitabatake (2008), 北畠 (2019) 総観気象学応用編

ET processes also show variation due to synoptic-scale conditions such as upper-level mobile troughs and preexisting fronts.

Schematic illustration of three ET types

Sea level pressure (contour)

Surface front

Upper-tropospheric jet stream
(gray arrow)

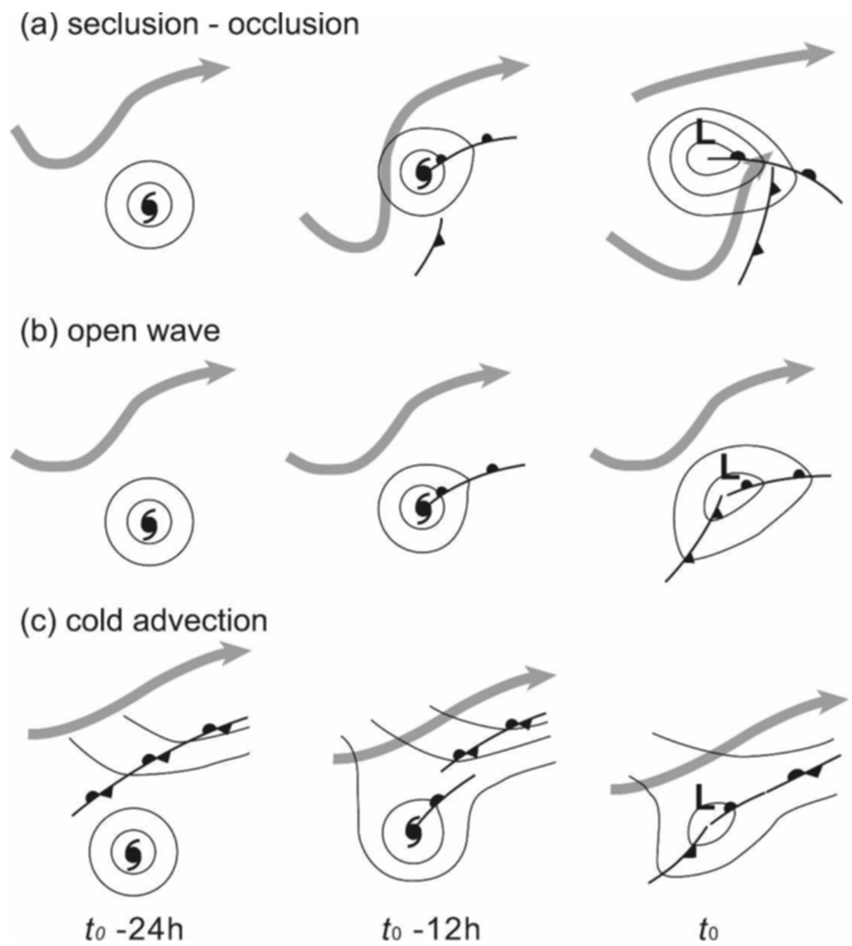

Kitabatake (2008), 北畠 (2019) 総観気象学応用編

[Summary]　5. Cyclone structures during ET

- Several characteristics are observed in many ET cases:
  warm frontogenesis, left-of-track precipitation, delta-shaped precipitation patterns, horseshoe-shaped wind patterns, and increase in area of strong wind.

- ET processes also show variation due to synoptic-scale conditions:
  upper-level mobile troughs and preexisting fronts.

6. An idealized experiment on ET

温低化の理想化実験

Experimental design

- Japan Meteorological Agency Non-Hydrostatic Model
  - Domain: 12,000 km (periodic) × 7,000 km (wall)
  - Horizontal grid spacing: 5 km
  - 5-class microphysics & KF cumulus scheme
- Zonally-uniform baroclinic zone
  - Temperature: tanh(y) distribution centered at y = 4500 km (Kirshbaum et al. 2018)
  - SST: 1°C higher than surface air temperature
  - The environment parameter is similar to that during Typhoon Hagibis (2019)
- A β-plane approximation for 45°N centered at y = 4500 km
- Initial disturbance: an axisymmetric vortex (maximum wind of 20 m s^{-1} at y = 1500 km)

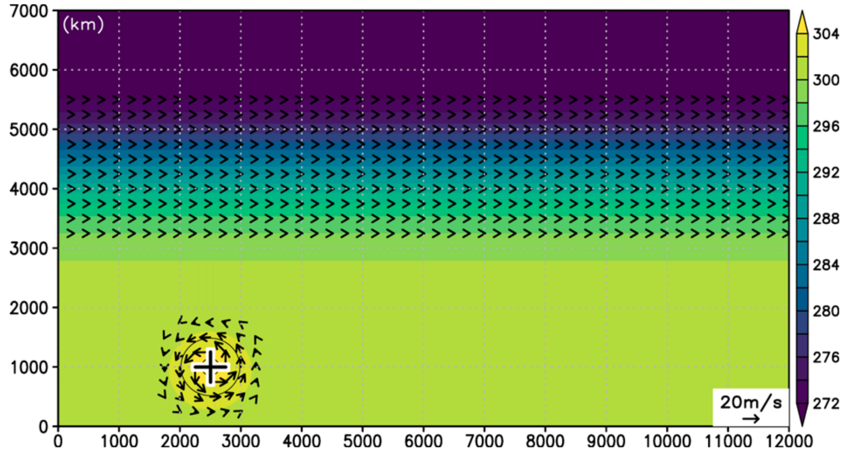

Initial fields at z=500 m: horizontal wind vectors, potential temperature (shading).

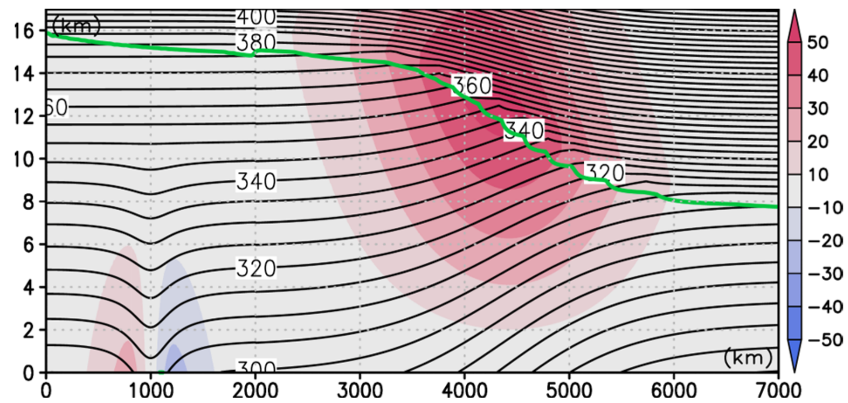

Meridional section through the cyclone center: zonal wind (shading), tropopause (2 PVU, green curve), potential temperature (black contour).

Track, precipitation, and intensity

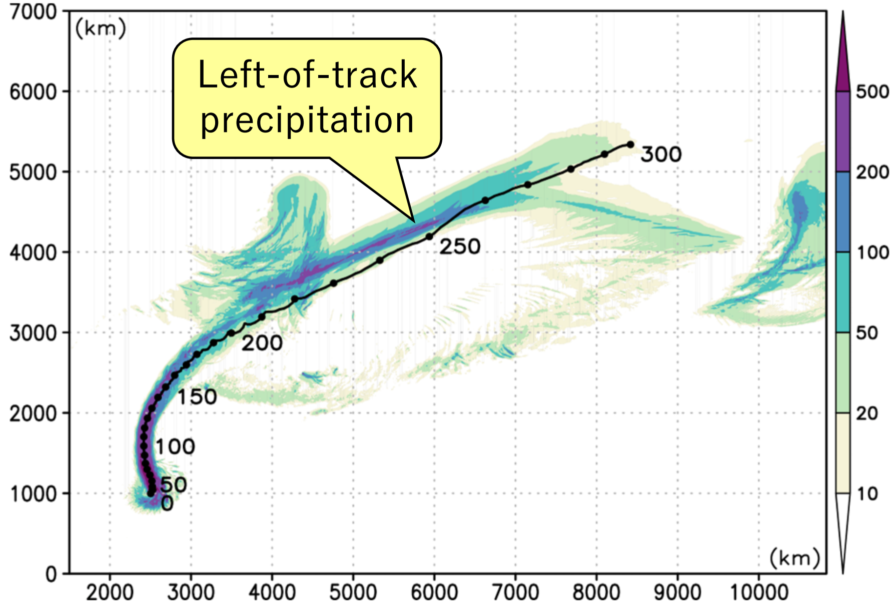

Total precipitation (mm; shading)
Cyclone track (black curve)
Digits denote integration time

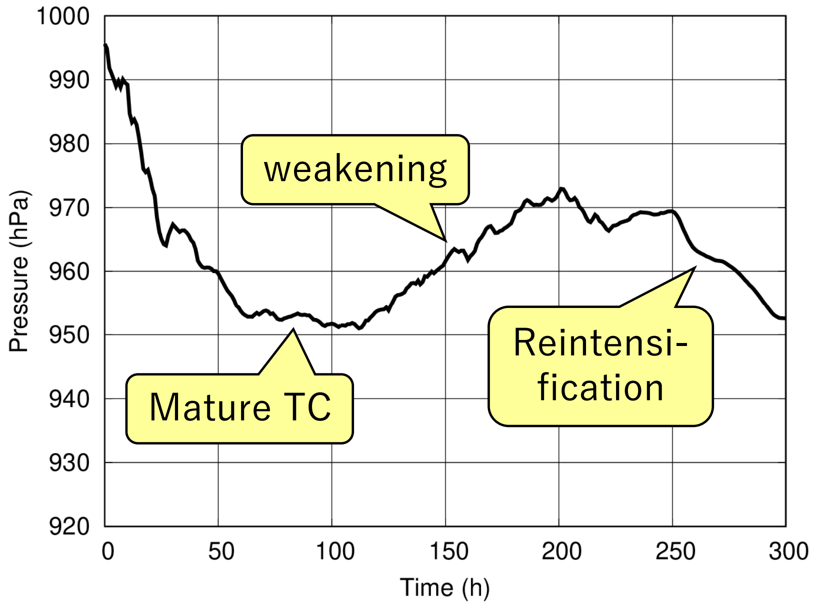

Minimum pressure

The beginning and end of ET based on the CPS analysis.

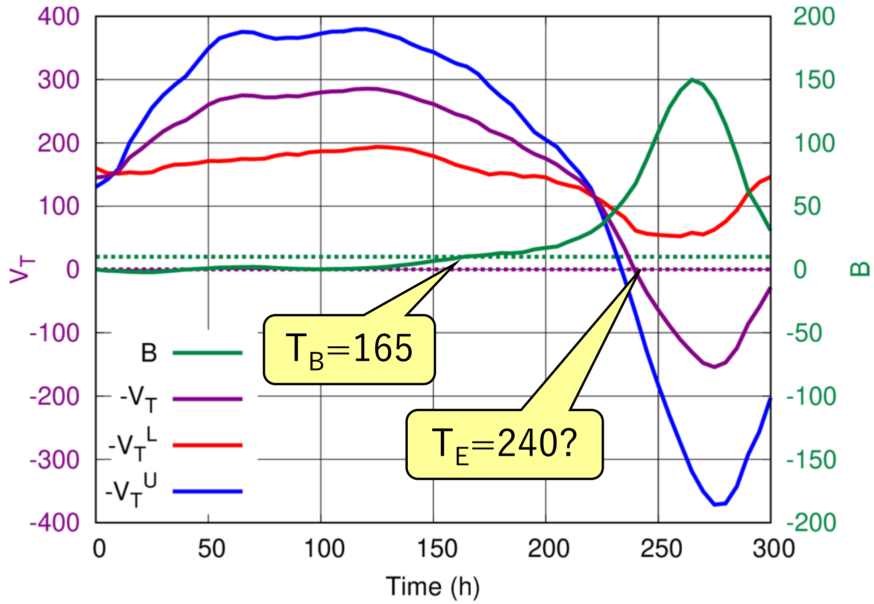

Total precipitation (mm; shading)
Cyclone track (black curve)
Digits denote integration time

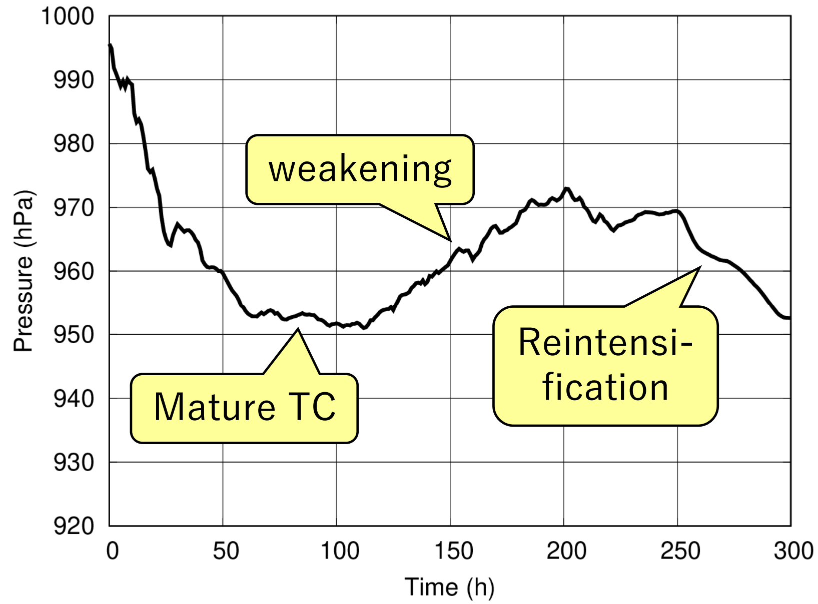

Minimum pressure

Although $-V_T^L$ decreases during ET, it never become negative.
Therefore, we use $0.5*(-V_T^L-V_T^U)$ for the definition of ET end (T_E),

Evolution of precipitation pattern

Total condensed water path
(shading; kg m^{-2})
Potential Temperature at z=500 m
(contour; every 4 K)

80 h TC
160 h Early ET
220 h Late ET
260 h EC
(T_B=165 h, T_E=240 h)

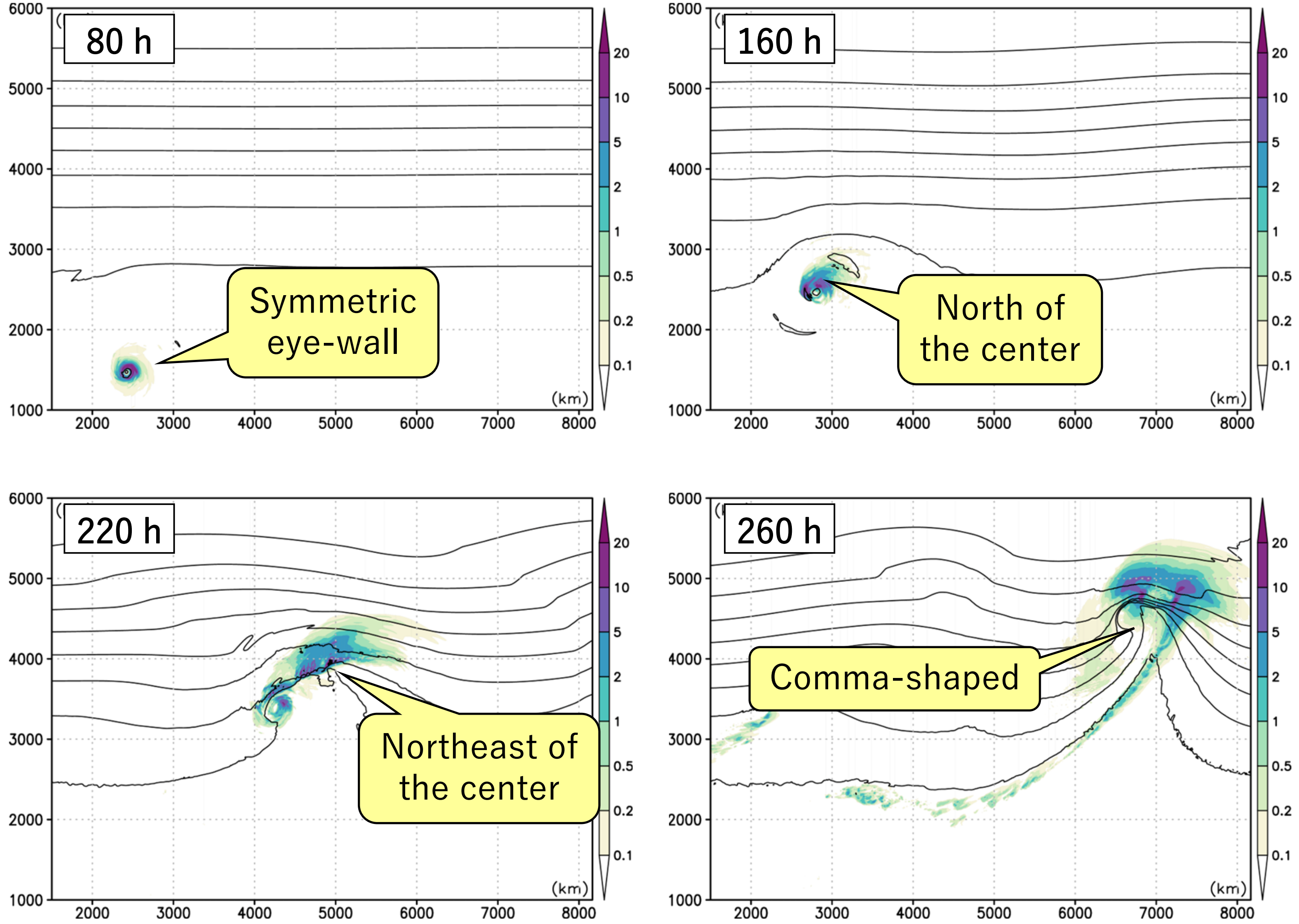

Evolution of upper tropospheric flow

Horizontal wind speed at z=10 km
(shading; m s^{-1})
Horizontal wind vectors
Cyclone center (+)

80 h TC
160 h Early ET
220 h Late ET
260 h EC
(T_B=165 h, T_E=240 h)

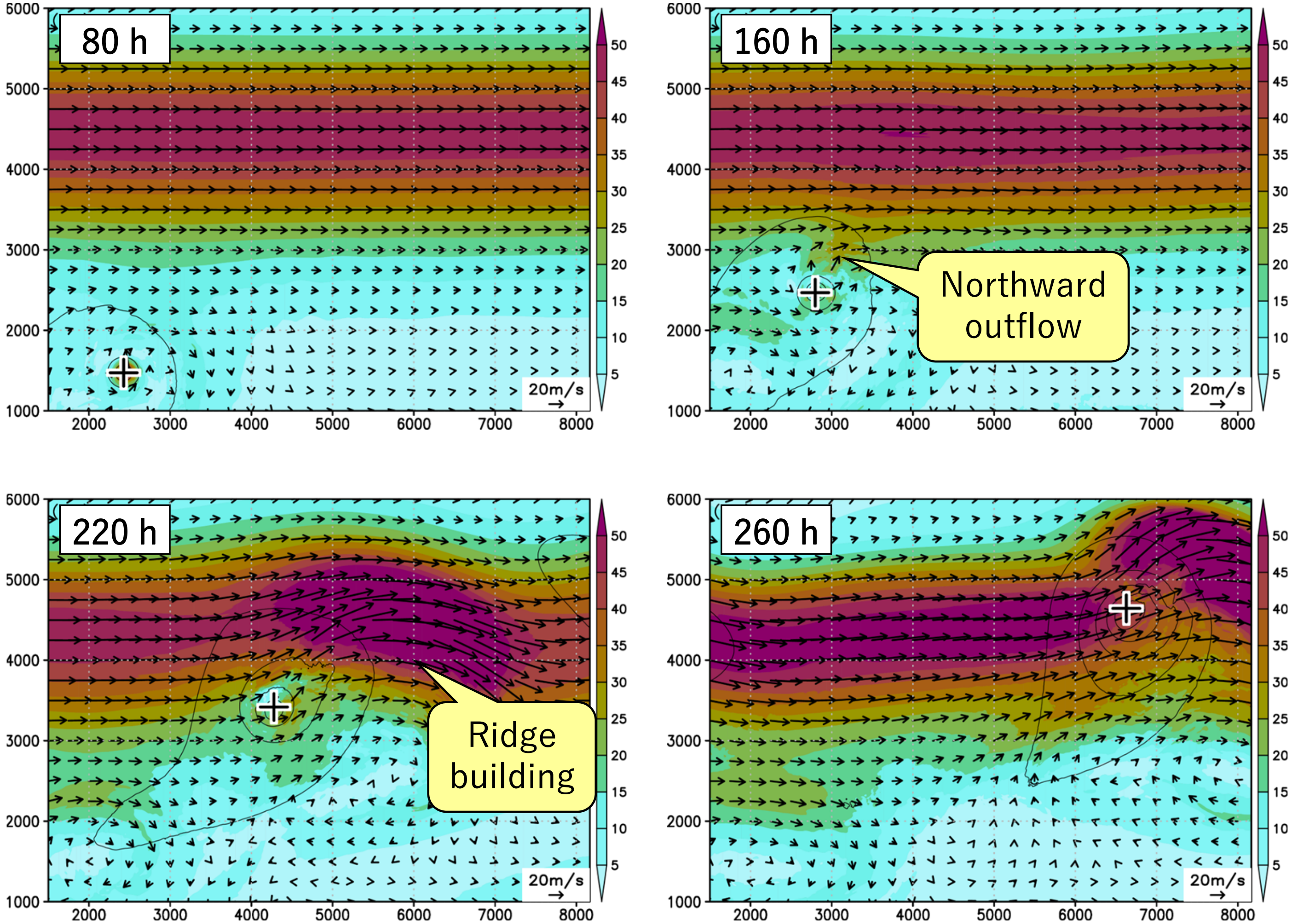

The areas of intense wind and precipitation increase during and after ET [A,B].

80 h TC
160 h Early ET
220 h Late ET
260 h EC
(T_B=165 h, T_E=240 h)

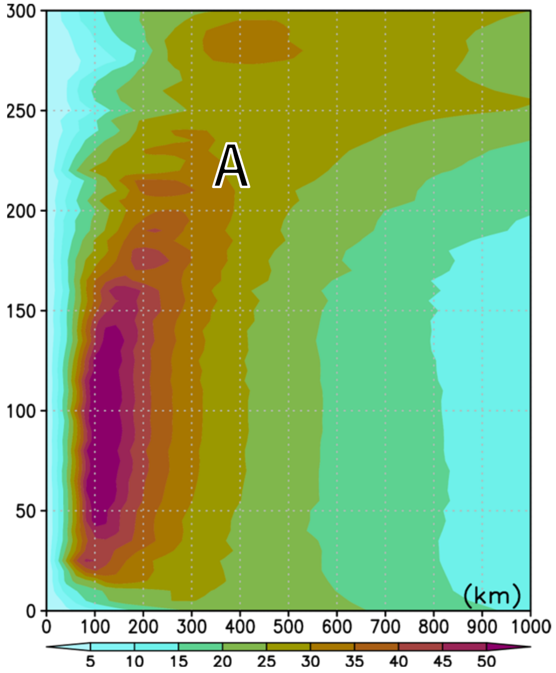

Tangential wind at z=10 m
(shading; m s^{-2})

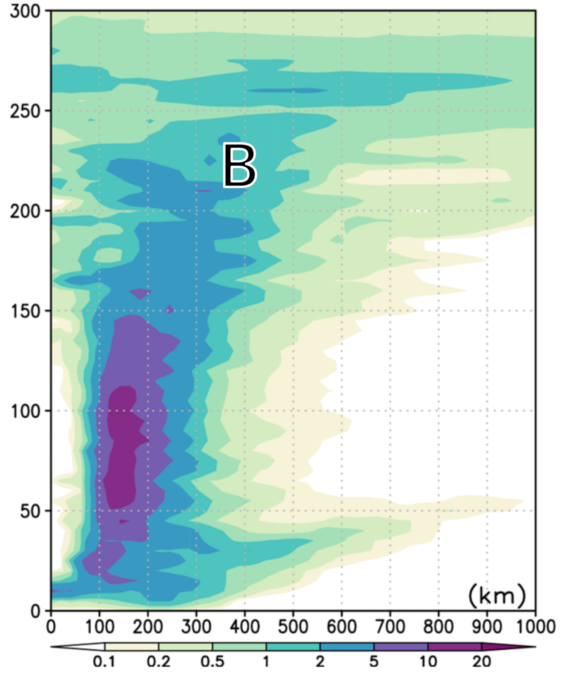

Total condensed water path
(shading; kg m^{-2})

Radius-time diagram of azimuthally averaged fields

[Late ET; 220 h] A warm front (A) northeast of the cyclone center causes an asymmetric precipitation pattern (B) and a horseshoe-like wind pattern (C).

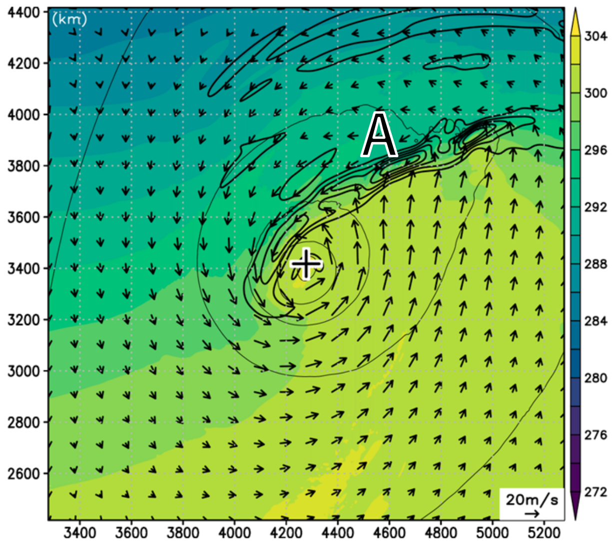

Potential Temperature at z=500 m
(shading; K)
Horizontal gradient of P.T.
(thick contour; 1 K $(10\ \mathrm{km})^{-1}$)

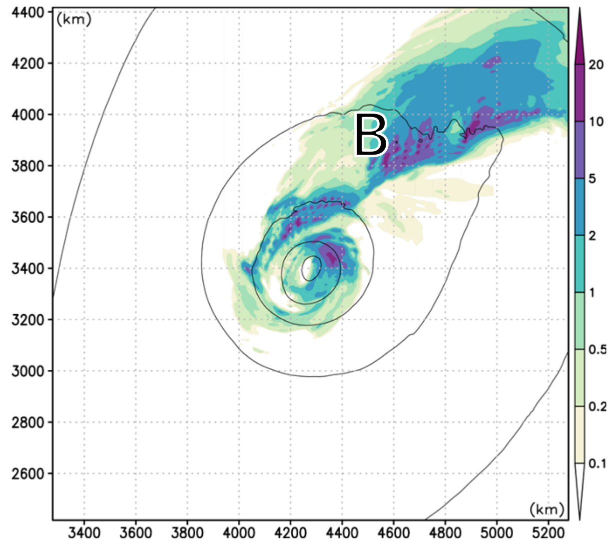

Total condensed water path
(shading; kg m^{-2})

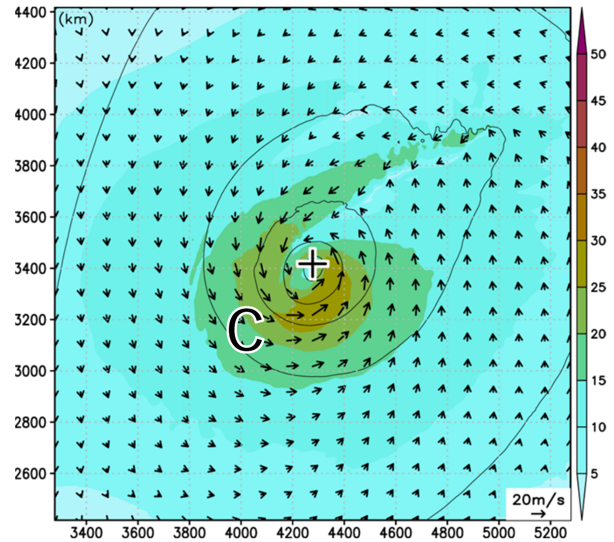

Wind speed at z=10 m
(shading; m s^{-1})
Horizontal wind vector

All figures: Sea level pressure (thin contour); Cyclone center (+)

The scholar frontogenesis

$$\frac{d}{dt}|\nabla_h\theta| = \frac{1}{2}|\nabla_h\theta|E\cos 2\beta - \frac{1}{2}|\nabla_h\theta|(\nabla_h \cdot V_h) - \frac{\partial\theta}{\partial z}\left(\nabla_h w \cdot \frac{\nabla_h\theta}{|\nabla_h\theta|}\right) + \nabla_h Q \cdot \frac{\nabla_h\theta}{|\nabla_h\theta|}$$

Deformation (nondivergent) — Divergence — Tilting (vertical advection) — Diabatic

$$E = \left[\left(\frac{\partial u}{\partial x} - \frac{\partial v}{\partial y}\right)^2 + \left(\frac{\partial v}{\partial x} + \frac{\partial u}{\partial y}\right)^2\right]^{\frac{1}{2}}$$

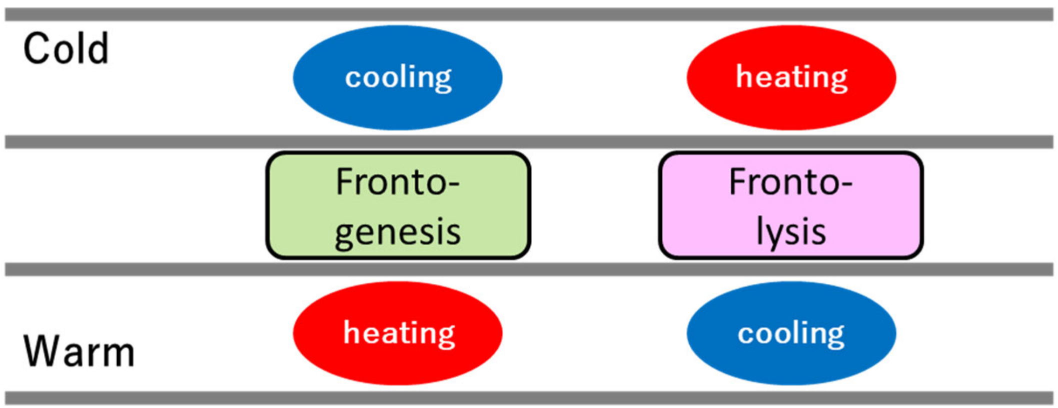

The deformation effect

Horizontal wind (black vectors)
Dilatation axis (gray line segments)
Isoline of θ (dotted line)
Frontogenesis (green)
Frontolysis (purple)

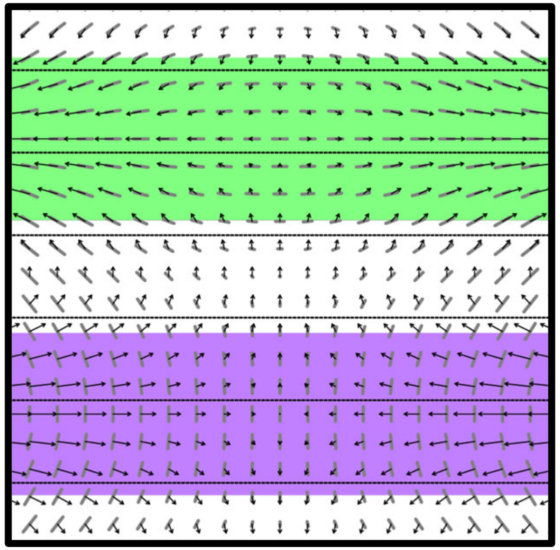

Dilatation axes oriented in the zonal and meridional direction. $\partial\theta/\partial y$ is uniform.

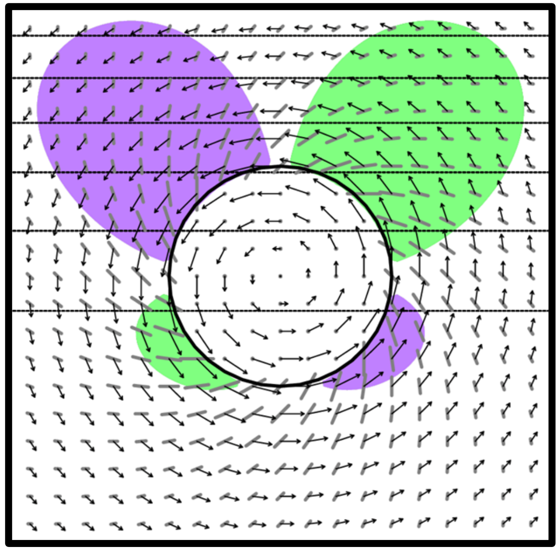

Dilatation axes associated with the Rankine vortex. $\partial\theta/\partial y$ is steep in the northern region.

Warm frontogenesis [(A)] occurs northeast of the center due to the deformation effect [(B,C)] (consistent with simple frontal dynamics).

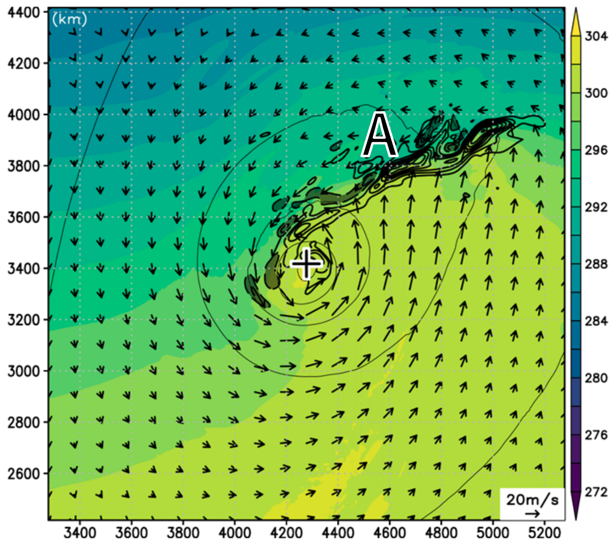

Total effects

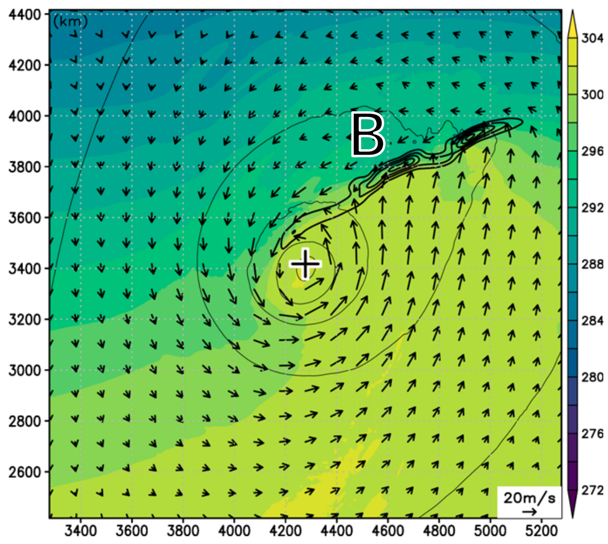

Deformation

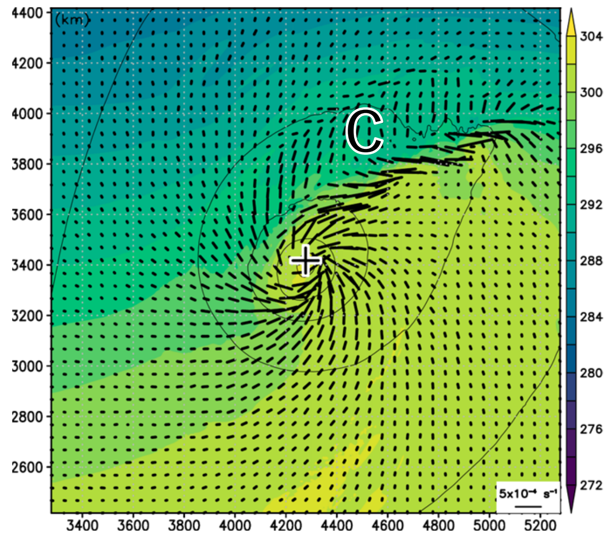

Dilatation Axis

Potential temperature (shading) and horizontal wind vector at z=500 m
Frontogenesis (solid contours every 2 × 10^{-8} K m^{-1} s^{-1})
Frontolysis (dashed contours every 2 × 10^{-8} K m^{-1} s^{-1} with shading)
Cyclone center (+)

The warm frontogenesis is enhanced by divergence and diabatic effects (A, C), while it is weakened by tilting effect (B). (feedback from vertical motion)

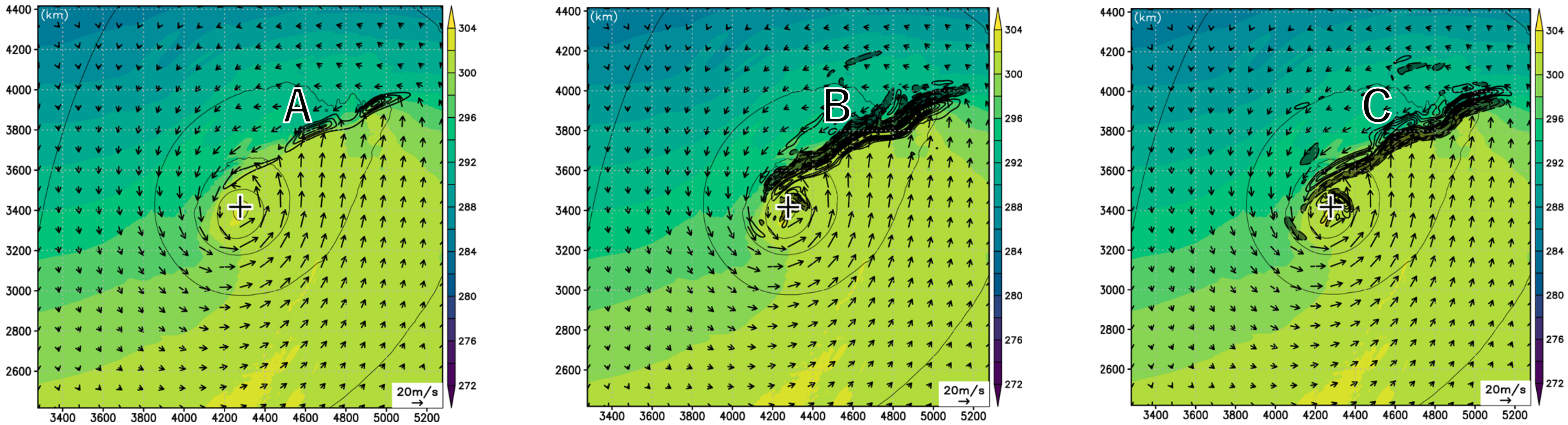

Divergence Tilting Diabatic

Potential temperature (shading) and horizontal wind vector at z=500 m
Frontogenesis (solid contours every 2×10^{-8} K m^{-1} s^{-1})
Frontolysis (dashed contours every 2×10^{-8} K m^{-1} s^{-1} with shading)
Cyclone center (+)

[Early ET; 160 h] Intense convection north of the cyclone center are associated with a delta-shaped rain region (A) and northward outflow (B).

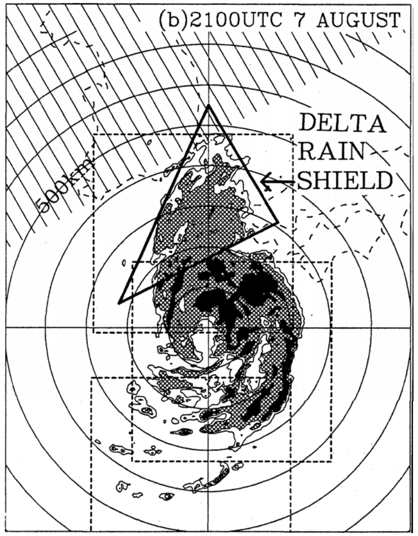

Delta-shaped rain region
(Shimazu 1998)

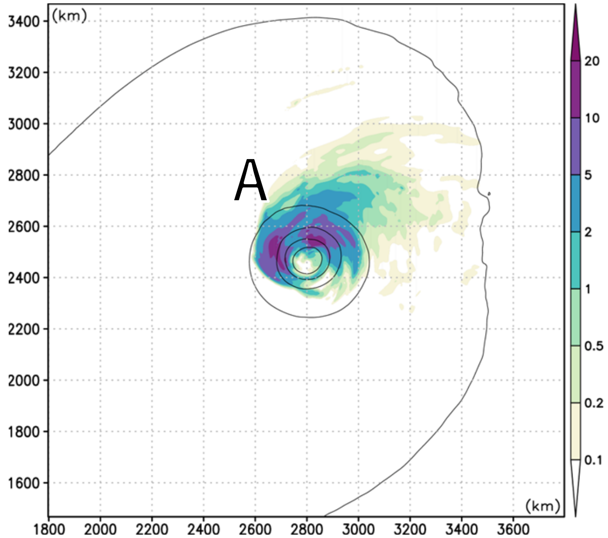

Total condensed water path
(shading; kg m^{-2})

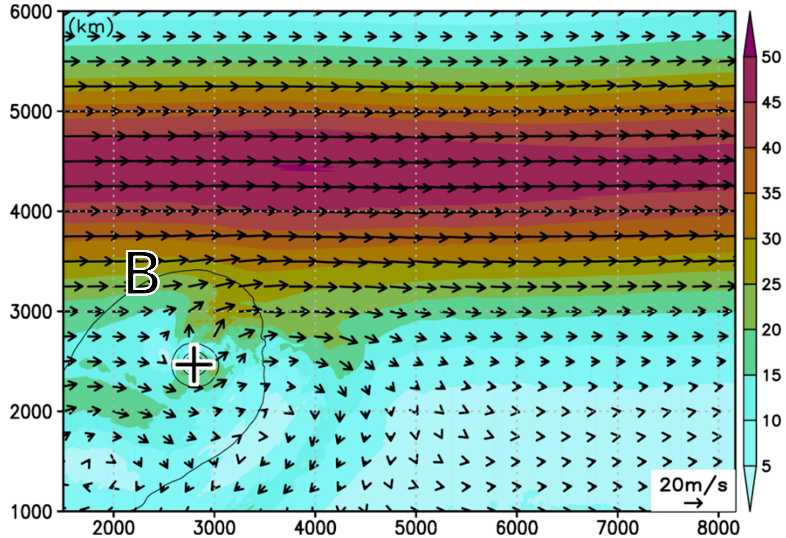

Horizontal wind speed at z=10 km
(shading; m s^{-1})
Horizontal wind vectors
Cyclone center (+)

Northward slantwise convection along the isentropic surface (A, B) is enhanced north of the cyclone center.

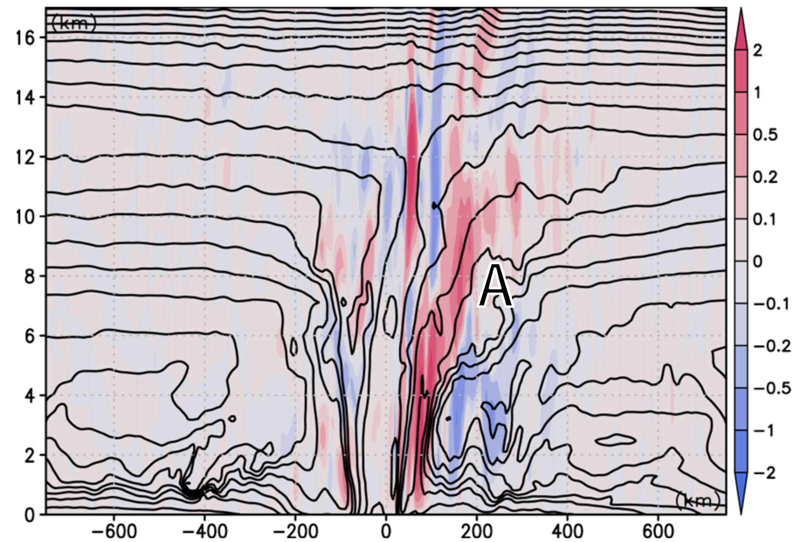

Vertical wind
(shading; m s^{-1})
Equivalent potential temperature
(contour; every 5 K)

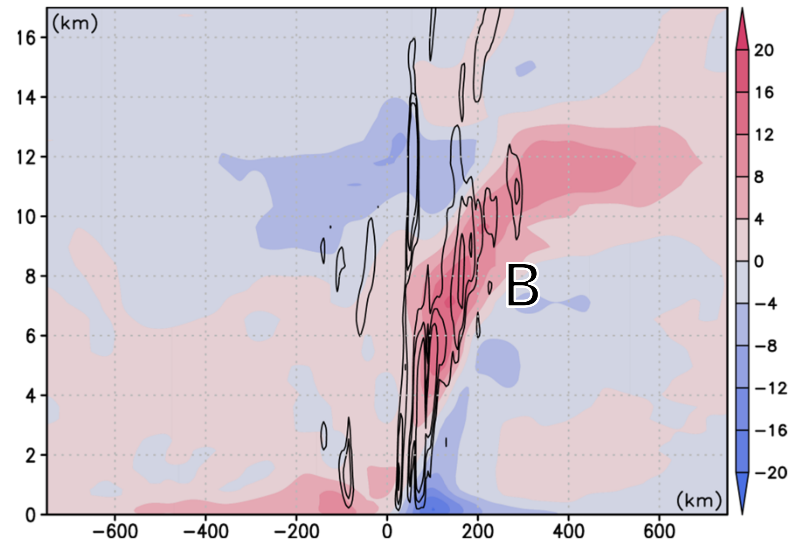

Meridional component of divergent wind
(shading; m s^{-1})
Ascending motion
(contour; 0.2, 0.5, 1 m s^{-1})

Meridional-vertical cross section through the cyc
(Horizontal axis indicates the distance from the cy

Symmetric instability is enhanced.
(Beyond the scope of the introduction)

[Summary]　6. An idealized experiment on ET

- Several characteristics of ET are reproduced in a simple experiment:
  warm frontogenesis, left-of-track precipitation, delta-shaped precipitation patterns, horseshoe-shaped wind patterns, and increase in area of strong wind.

- There are also some discrepancies between the idealized and real world:
  slow northward motion and evolution, a persistent TC intensity and low-level warm core.

  ➔ These may be attributed to missing factors:
  e.g., upper-level troughs and subtropical high pressure systems.

[Summary]　All topics

- Various types of cyclones including hybrid cyclones form around the globe.
- ET has a beginning and an end.
- The CPS express the continuous nature of types and transitions of synoptic-scale cyclones, and has been widely used as an objective cyclone classification method.
- The ET season is later than the TC season because of larger baroclinicity in autumn.
- Several characteristics are found in many cases and in an idealized experiment: warm frontogenesis, left-of-track precipitation, delta-shaped precipitation patterns, horseshoe-shaped wind patterns, and increase in area of strong wind.
- ET processes have a variation partly due to synoptic-scale conditions: upper-level mobile troughs and preexisting fronts.